UNIVERSIDADE DE SÃO PAULO

CENTRO DE ENERGIA NUCLEAR NA AGRICULTURA

EDUARDO SANTOS RODRIGUES

Uptake and phytotoxicity of lanthanum and cerium by soybean (*Glycine max* L.)

Piracicaba

2019

EDUARDO SANTOS RODRIGUES

Uptake and phytotoxicity of lanthanum and cerium by soybean

(*Glycine max* L.)

Versão revisada de acordo com a Resolução CoPGr 6018 de 2011

Dissertation presented to Center for Nuclear Energy in Agriculture of the University of São Paulo as a requisite to the Ms.Sc. Degree in Sciences

Concentration Area: Chemistry in Agriculture and Environment

Advisor: Prof. Dr. Hudson Wallace Pereira de Carvalho

Piracicaba

2019

Dados Internacionais de Catalogação na Publicação (CIP)

Seção Técnica de Biblioteca - CENA/USP

Rodrigues, Eduardo Santos

Absorção e fitotoxicidade de lantânio e cério pela soja (*Glycine max* L.) / Uptake and phytotoxicity of lanthanum and cerium by soybean (*Glycine max* L.) / Eduardo Santos Rodrigues; orientador Hudson Wallace Pereira de Carvalho. - - Versão revisada de acordo com a Resolução CoPGr 6018 de 2011. - - Piracicaba, 2019.

76 p. : il.

Dissertação (Mestrado – Programa de Pós-Graduação em Ciências. Área de Concentração: Química na Agricultura e no Ambiente) – Centro de Energia Nuclear na Agricultura da Universidade de São Paulo, 2019.

1. Adubação foliar 2. Cério 3. Espectrometria de massas 4. Espectroscopia por fluorescência de raios X 5. Fitotoxicidade 6. Lantânio 7. Nanopartículas 8. Soja 9. Terras raras I. Título

CDU (632.95.024 + 633.34) : 543.42

Elaborada por:
Marilia Ribeiro Garcia Henyei
CRB-8/3631
Resolução CFB Nº 184 de 29 de setembro de 2017

ACKNOWLEDGMENTS

First, I would like to thank two people that made this work possible, Prof. Hudson Wallace Pereira de Carvalho for believing and supporting me and for making my trip to Canada possible and Dr. Eduardo de Almeida by experience and knowledge transmitted to me and for his patience, and support. Both contributed a lot to my personal and professional development during this 4-year together.

I would like to thank the Center for Nuclear Energy in Agriculture (CENA) and all employees of this institution, the University of São Paulo (USP) for the opportunity and for providing me with all the necessary facilities to develop this work. I am also very grateful to the São Paulo Research Foundation - FAPESP (Process Nº 2017/16375-4) and National Council for Scientific and Technological- CNPq (Process Nº 134288/2017) for granting the scholarship.

I would like to thank my fellow Post Doc, PhD, Masters and Undergraduate students at the Laboratory of Nuclear Instrumentation (LIN) João Paulo Rodrigues Marques, Joyce R. P. Santos, Geovani T. Costa Jr, Marcos H. F. Gomes, Rafael G. de Lima, Bianca A. Machado, Sara L. Z. Romeu, Gabriel S. Montanha, and Antônio C. S. Mendes for the friendship, cooperation and companionship during the development of this work.

I would like to thank the Brazilian Synchrotron Light Laboratory (LNLS) for beamtimes at XAFS2 (Proposal Nº 20180725) beamlines and the beamlines scientists Dr. Carlos A. Perez and Dr. Santiago Figueroa for their support during the XAS measurements.

I would like to thank to prof. Rafael Santos for welcoming me to University of Guelph in Canada and his research assistant Hugo Fantucci.

ABSTRACT

RODRIGUES, E. S. **Uptake and phytotoxicity of lanthanum and cerium by soybean (*Glycine max* L.)**. 2019. 76 p. Dissertação (Mestrado em Ciências) – Centro de Energia Nuclear na Agricultura, Universidade de São Paulo, Piracicaba, 2019.

Although not essential for plants the lanthanum and cerium elements, both rare earth element (REE), have received attention due to increased use in industry and their potential impact on environment and agriculture. Regarding agriculture in Brazil, phosphate fertilizer shows REE in its composition depending on the raw material used and process of purification. This study aimed at investigating the effect of La and Ce on the development and production of *Glycine max* L. Foliar application of aqueous solutions of La^{3+} and Ce^{3+} nitrates on soybean plants was sprayed at 200 and 2,000 mg L^{-1}. The foliar treatments did not affect the development and production. However, the treatments induced phytotoxicity since foliar injuries appeared after the spraying. Microprobe X-ray fluorescence spectroscopy combined to scanning electron microscopy and X-ray absorption near edge structure was used to investigate the phytotoxic effect. In another approach, CeO_2 nanoparticles (NPs) were applied on roots at 0.062 and 0.933 μg kg^{-1} both concentrations were predicted to occur by the year 2050. Ce nitrate translocation from root to shoot was time-dependent. On the other hand, no difference in uptake rate was found for CeO2 NPs treatment over a period of four weeks. Single particle inductively coupled plasma mass spectrometry analysis detected Ce NPs in the shoots of soybean with an average size higher than was applied (60.3 nm). All results presented here provide evidence that soybean can take up and translocate La soluble from shoot to grain, and Ce in the soluble and NPs forms from roots to shoot and grains, highlighting the concerns regarding the introduction of REE in the food chain.

Keywords: Rare earth elements. Agriculture. Lanthanides. Leaf fertilization. X-ray fluorescence spectroscopy.

RESUMO

RODRIGUES, E. S. **Absorção e fitotoxicidade de lantânio e cério pela soja (*Glycine max* L.)**. 2019. 76 p. Dissertação (Mestrado em Ciências) – Centro de Energia Nuclear na Agricultura, Universidade de São Paulo, Piracicaba, 2019.

Embora não sejam essenciais para as plantas os elementos de terras raras (ETR) receberam grande atenção devido ao aumento do uso pela indústria e consequentemente seu potencial impacto no ambiente e na agricultura. No que diz respeito à agricultura no Brasil, os fertilizantes fosfatados apresentam REE em sua composição, dependendo da matéria-prima utilizada e do processo de purificação. Dessa forma, este estudo objetivou investigar os efeitos de La e Ce no desenvolvimento e produção de *Glycine max* L. Para tal, aplicações foliares de soluções aquosas de nitratos de La^{3+} e Ce^{3+} foram feitas nas doses de 200 e 2.000 mg L^{-1}. Os tratamentos foliares não afetaram o desenvolvimento das plantas e a produção. No entanto, os tratamentos induziram fitotoxicidade, uma vez que surgiram lesões foliares após a pulverização. A espectroscopia por fluorescência de raios X combinada com a microscopia eletrônica de varredura e a espectroscopia de absorção de raios X foram usadas para investigar os efeitos fitotóxico. Em outra abordagem, nanopartículas de Ce (NPs) foram aplicadas via raiz nas concentrações 0,062 e 0,33 μg kg^{-1}, ambas as concentrações estão previstas para ocorrer no ano de 2050. A translocação de nitrato de Ce da raiz para a parte aérea foi dependente do tempo de exposição. Por outro lado, não foi encontrada diferença na taxa de absorção no tratamento com CeO_2 NPs durante um período de quatro semanas. A análise por single particle inductively coupled plasma mass spectrometry detectou Ce NPs no tecido foliar da soja com tamanho médio superior ao aplicado (60,3 nm). Todos os resultados apresentados aqui evidenciam que a soja é capaz de absorver e translocar La da parte aérea para os grãos e Ce nas formas solúvel e NPs das raízes para parte aérea e grãos. Assim destaca-se a preocupação com a introdução de ETR na cadeia alimentar.

Palavras-chave: Elementos terras raras. Agricultura. Lantamídeos. Adubação foliar. Espectroscopia por fluorescência de raios X.

FIGURE LIST

TABLE LIST

SUMMARY

1. INTRODUCTION

1.1 Rare Earth Elements: Chemistry

Rare Earth Elements (REE) comprise 17 elements encompassing all 15 lanthanides and also including scandium (Sc) and yttrium (Y) (DAMHUS; HARTSHORN; HUTTON, 2005). The majority of REE belongs to the F-block of the periodic table and the most common oxidation state is +3, although cerium (Ce) and europium (Eu) can also be found as +2 and +4. In fact, the "rare earth" denomination comes from the names that were given to metal oxides and due to the previous idea of scarcity of these elements in Earth's crust. However, nowadays it is known that the REE concentrations are higher than other known elements (ABREU, 1991; FINK, 2005). For example, the rarest REE is around two hundred times more abundant than gold (Au).

The increase in demand of REE has been reflected in the annually production that have an increase of *ca*. 55% in the period of 2013 to 2018 (USGS, 2013; 2019). In addition, the average compound annual growth rate for REE is estimated to be 13.7 % between 2017 and 2021 (WEALTH DAILY, 2016). The yearly global consumption of rare-earth oxides is estimated in 150,000 tons, a market at US$ 9 billions (GANGULI; COOK, 2018).

Regarding the natural occurrence of REE, they are generally found in rocks associated to other ores, such as monazite (REE-PO_4) and bastnaesite (REE-CO_3F) are two of the main sources of REE (FINK, 2005). According to 2016's US Geological Survey, the largest REE reserves are found in China (36%), Brazil and Vietnam (18% each), Russia (10%), India (6%), United States (1%) and other countries (11%). Not surprisingly, the worldwide production has been dominated by China that accounts for nearly 70% (USGS, 2019). On the other hand, Brazil has 0.6% share on production of REE as stated in the same report (USGS, 2019).

Besides that, an important issue regards the potential impact of REE's on the environment and agriculture (ZHUANG et al., 2017). Rare earth elements have been included in the "New and Emerging Risks to Occupational Safety and Health" by the European Agency for Safety and Health at Work. Regarding European Agency for Safety and Health at Work (2013), phosphate fertilizer shows REE in its composition (concentration is depending of raw material used) (RAMOS et al., 2016). There are also reports that REE have been deliberated applied as to fields in Chinese agriculture (TURRA, 2018). Thus, more investigation of REE effects on the agriculture and way of REE enter in chain food are needed.

1.2 La and Ce in agriculture plant metabolism

REE have been used for decades as beneficial elements in Chinese agriculture (PANG; LI; PENG, 2001). However, textbooks of mineral nutrition of plants do not even appoint REE as beneficial elements. The second edition of the classic "Mineral Nutrition of Higher Plants", by Horst Marschner, dedicated only one paragraph to Ce and La in page 268 (MARSCHNER, 2011). The author highlighted that such elements have been used in China for a long time and that they can lead to higher crop yields. Despite of that, no deeper discussion about their function and role are given.

The most common application methods consist of either seed treatment or foliar spraying. They can be applied as nitrates, phosphates or chlorides. Commercial products such as Azomite^{TM} and HappyHan Green^{TM} are easily found on Chinese market. The evaluation of the outcome yield increase after spreading REE on crops is scarce. It has been reported a yield increase for wheat (*Triticum aestivum*) by 4-10%, onions (*Allium cepa*) 13-14%, eggplant (*Solanum melongena*) 23-45%, corn (*Zea mays*)6-12%, potato (*Solanum tuberosum*) 10-14%, among others (PANG; LI; PENG, 2001). Despite such exciting figures, the mechanisms behind this improvement are far from being understood.

Among the effects of La and Ce on biological processes of plants, some authors report that they can influence photosynthesis rate, replace the Mg^{2+} of chlorophyll molecules, accelerate the change of protochlorophyll to chlorophyll and stimulate the enzymes involved in its synthesis (FASHUI et al., 2002; HONG, 2002).

The correlation between the absorption of La and other elements have been also discussed in the literature ((FASHUI et al., 2002; HONG, 2002; SHYAM; AERY, 2012; YIN et al., 2009; ZENG et al., 2000)). Yin et al. (2009) verified that the effect of Mg^{2+} deficiency can be ameliorated with La^{3+} or Ce^{3+}, and still, the same authors demonstrated plant development improving and higher photosynthetic net rate for plants exposed to both elements (YIN et al., 2009).

Besides the Mg^{2+} ion, La and Ce can replace Ca^{2+} ion in biomolecules. This replacement comes from the similarity in their ionic radius (Ca^{2+} ionic radius is 180 pm, La 195 pm and Ce 185 pm) (FASHUI et al., 2002; FINK, 2005; HONG, 2002; SHYAM; AERY, 2012). Foliar treatment with La reduces Ca content, thus seemingly La^{3+} may replace Ca^{2+}. In principle, they may have the same carriers and simply compete for transporter sites. However, further investigation is required. Diatloff, Asher and Smith (1999b) evaluated the effect of REE on the growth and nutrition of *Vigna radiate* L. and *Zea mays* L. Phytotoxicity and bioaccumulation

of REE were demonstrated even at low concentrations and suggested no beneficial biological effect for REE in plants.

Fashui et al. (2002) studied the effect of the content of REE on spinach (*Spinacia oleracea*) grown in hydroponic solution. It was reported higher mass gain and chlorophyll concentration in addition to superior net rate of photosynthesis. These effects were attributed to an increment of synthesis of chlorophyll molecule precursors and, consequently, a superior nitrogen and phosphorus intake. In addition, the treatment of corn seeds with Ce caused an increase in germination and vitality. This increase was associated with greater enzymatic response of α-amylase, responsible for degrading the starch in endospermic seeds (ESPINDOLA; DE MENEZES; BARBIERI, 2013).

It seems that Ce and La can promote plant growth in low concentrations, although the biological mechanism is not clear. In excess, however, they may cause oxidative stress. The typical range of accumulation is 0.15-0.55 mg kg^{-1} and the most common species are Ce^{3+}, $CeOH^{2+}$, La^{3+} and $LaOH^{2+}$ (DJINGOVA et al., 2013).

1.3 Soybean

Soybean was chosen as a model plant herein because of its worldwide importance. Soybean is used for oil production, and as a vegetal protein source for animal and human feed. According to the United States Department of Agriculture (DUKHNYTSKYI, 2019) soybean was ranked in fourth place in the global grain production and in acreage in the years 2018/2019. During this period crop yield reached 362 million metric tons and acreage achieve 125 million of hectares (DUKHNYTSKYI, 2019).

Soybean has great economic importance in Brazil. Charactered by its data of production and exportation featuring as the largest soybean exporter in the world (itself represented 56% in the global exportation) and the second largest producer (114 million tons), only behind the USA 123 million tons). Soybean fields occupy 31.90 mi ha, out of the 57.66 mi hectare cultivated countrywide, or 55.3% of the total area planted for grains. All data are the 2018/2019 crop. (EMBRAPA, 2019).

1.4 Hypothesis

This study raised the following hypothesis:

i) Rare earth elements (lanthanum and cerium) can promote or inhibit the plant growth (*Glycine max* L.)

ii) *Glycine max* L. can take up and translocate rare earth elements (lanthanum and cerium) from leaf to grain

iii) *Glycine max* L. can take up and translocate cerium oxide nanoparticle from root to grain

1.5 Objectives

The general objective of this master's dissertation was to assess the effect of REE (La and Ce) on the plant development of Soybean (*Glycine max* L.) and to verify whether these elements could be absorbed and translocated within the plants.

1.5.1 Specific goals

On Chapter 2 the specific goals are:

i) To develop formulations for foliar application of aqueous solution containing Ce and La;

ii) Evaluate the effects of higher concentration of Ce and La on the plant development;

iii) Characterization of phytotoxic effect on the leaf;

iv) Evaluate the effects of Ce and La treatments on the plant development;

v) To quantify the incorporated La in the grain by the soybean;

On Chapter 3 the specific goals are:

i) Determine Ce concentration on shoot and grains of plants

ii) Determine the average size of Ce NPs in shoot of plants using Single particle inductively coupled plasma mass spectrometry,

iii) Perform kinetic studies to measure the Ce uptake rate;

iv) Evaluate the effects of Ce NPs on the plant development.

1.6 Structure of the dissertation

This dissertation comprises an introductory text followed by two chapters. First chapter comprises a manuscript published by the *Journal Rare Earth Element*. The second chapter will be submitted to Environment Science & Technology journal with title “Effect of nano cerium oxide on soybean (*Glycine max* L.) crop: a perspective towards its 2050’s concentrations”.

The original texts were adapted to comply with institutional format requirements.

Chapter 1: Rodrigues, E. S et al. Foliar application of rare earth elements on soybean (*Glycine max* L.): Effects on biometrics and characterization of phytotoxicity. J. Rare Earth, 2019.

2 FOLIAR APPLICATION OF RARE EARTH ELEMENTS ON SOYBEAN (*GLYCINE MAX* L.): EFFECTS ON BIOMETRICS AND CHARACTERIZATION OF PHYTOTOXICITY

Abstract

This study aimed at investigating the effects of foliar application of aqueous solutions of La^{3+} and Ce^{3+} nitrates on soybean plants (*Glycine max*). First, we observed that triton HW 1000 surfactant at 0,01% (v/v) reduced droplets contact angle and increased their drying time. Under greenhouse conditions, the foliar treatments did not affect chlorophyll content, plant height, number of leaves, number of pods, number of seeds per pod and average seed weight. However, the treatments induced phytotoxicity since foliar injuries appeared after the spraying. Microprobe X-ray fluorescence spectroscopy combined to scanning electron microscopy showed that the leaf lesions were positively correlated to accumulation of Ce and La on the leaf surface and also promotes structural alteration to the epidermal cells. X-ray absorption near edge structure showed the La and Ce nitrates were partially bio transformed into oxides by the leaves which might explain the harmful effects.

Keywords: Leaf fertilization; rare earth elements; soybean; X-ray fluorescence spectroscopy; X-ray absorption spectroscopy

2.1 Introduction

Although REE have been mostly in the spotlight due to the high technological application (GANGULI; COOK, 2018), the REE use in agriculture as plant fertilizer (REN et al., 2016) and stimulator (AGATHOKLEOUS; KITAO; CALABRESE, 2018; DE OLIVEIRA et al., 2015) has recently drawn attention. Particularly, the effects of lanthanum on plants present hormetic dose-response behavior from stimulation to toxicity depending on the dose (AGATHOKLEOUS; KITAO; CALABRESE, 2018). Lanthanum administered by root under hydroponic growth at 5 and 10 μM increased photosynthetic rate, total chlorophyll, root and shoot biomass of soybean (*Glycine max*). On the other hand, a reduction of soybean growth was verified at concentration above 10 μM L^{-1} (DE OLIVEIRA et al., 2015).

Other REE used in agricultural context is cerium (ADISA et al., 2018; HONG; QU; WANG, 2017). It has been reported photosynthesis promotion and carboxylation efficiency enhancement for soybean seedling after Ce spraying (LIANG; HUANG; ZHOU, 2006). Similarly, Ce foliar application at 20 mg L^{-1} prevents UV-B-induced stress in soybean seedlings (TURRA, 2018). On the other hand, nano-Ce O_2 in high doses diminished the chlorophyll content, altered antioxidant enzymatic activities (ZHANG et al., 2017) and also cause toxic effects on root biomass (LI et al., 2014).

Table 2.1 shows a set of studies on the effects of foliar application of La and Ce on plants. In general, beneficial effects have been verified below 100 mg L^{-1} in foliar application for both elements, with a suitable concentration at 11 mg L^{-1} (Table 2.1). As shown in Table 2.1, the proper concentration for Ce requires further investigation. The beneficial and harmful effects are associated with alterations on the photosynthetic rate, electron transport chain, and resistance to biotic and abiotic stresses, reactive oxygen species (ROS) and activity of enzymes that operate in ROS (GAO et al., 2012). In the meantime, there are few publications that report their impacts on grain production (AGATHOKLEOUS; KITAO; CALABRESE, 2018; LIU et al., 2012).

The other side of the coin concerns the potential impact of REEs on the environment (ZHUANG et al., 2017), particularly in the nearby REEs mining region (CARVALHO, 2017). Furthermore, the REEs are included in the “New and Emerging Risks to Occupational Safety and Health” by the European Agency for Safety and Health at Work. Thus, new findings on the detrimental REEs effects on the environment are welcome (EUROPEAN AGENCY FOR SAFETY AND HEALTH AT WORK, 2013).

In view of the potential of La and Ce to boost plant productive performance, this study aimed to investigating the effects of foliar applied $La(NO_3)_3$ and $Ce(NO_3)_3$ solutions on soybean. First, the surfactant effects on the physical chemical properties in the foliar solution, namely contact angle and drying time, were evaluated. Then, we monitored the plant response by measuring chlorophyll, biomass and grain yield. Additionally, we employed microprobe X-ray fluorescence, SEM-EDX and X-ray absorption spectroscopy to shed light on understanding phytotoxicity caused by the REEs solutions.

2.2 Leaf absorption

The foliar fertilization (FF) is an effective method for correcting plant nutritional deficiencies in short period of time. Nowadays, this method has been fostered by technological advances (FERNÁNDEZ; SOTIROPOULOS; BROWN, 2015). The FF is based on the diffusion of nutrients via leaves. However, its effectiveness depends upon the penetration of the sprayed element (FERNÁNDEZ; SOTIROPOULOS; BROWN, 2015).

Several factors affect the efficiency of foliar absorption, namely the leaf anatomy and age, the nutrient (active ingredient), physicochemical properties of the solution and environmental factors such as temperature and air humidity (FERNÁNDEZ; SOTIROPOULOS; BROWN, 2015). The leaf anatomy contains physical barriers that protect the plants against water loss and entry of pathogens, which also constrain the nutrient entering. The main barrier is the cuticle, a waxy layer with a hydrophobic characteristic that covers the epidermis (RAVEN; EVERT; EICHHORN, 2014).

Regarding the foliar absorption pathways, some hypotheses have been raised and discussed in the literature. The trichomes present on the leaf epidermis have several functions, albeit it is still unclear whether they are involved in foliar absorption. The stomata are structures formed by differentiated epidermal cells, called guard cells, and these cells control the opening and closing of the stomatal crevices, where gas diffusion occurs. The diffusion of the active element in the solution by the stomata is still poorly understood, however it is known that this structure can contribute to absorption (RAVEN; EVERT; EICHHORN, 2014) .

Environmental factors can influence both the physiological processes of the plant, for instance the opening and closing of the stomata, as wells as the properties of the nutrient solution. To circumvent these effects adjuvants are added to the solutions (FERNÁNDEZ; SOTIROPOULOS; BROWN, 2015; HAZEN, 2000).

Additionally, the foliar absorption is regulated by the nutrient solubility, ionic diameter, hydratability, mobility and its metabolisation. Both latter ones are the main factors affecting its absorption by leaves. The free ion species are rapidly absorbed and are transported to other parts of the leaf and redistributed from the organ of residence to other parts of the plant (FERNÁNDEZ; SOTIROPOULOS; BROWN, 2015; HAZEN, 2000).

With regard to the speed of diffusion of ions, it increases as their ionic radius decreases, and vice versa. The hydratability affects the ion diffusion because of the hydration water layer: the higher the hydratability, the thicker is the layer. Thus, the hydrated ions diffuse less rapidly than the non-hydrated ones, taking into account the same diameter (FERNÁNDEZ; SOTIROPOULOS; BROWN, 2015).

As for the nutrient solution, adjuvants are substances added to the solution to change its chemical properties. In that sense, the humectants are added to retard the drying of the nutrient solution. The surfactant agent reduces surface tension and increases the area of contact with the leaf (HAZEN, 2000).

Table 2.1. Bibliographical survey on the foliar application of La and Ce and their effects on plants

References	Element and concentration (mg L^{-1})	Model plant	Application method	Effects
(ZHU et al., 2018)	La, 5- 16	*Lavandula angustifolia*	Plant at six leaf stage were sprayed with La solution 3 times for 3 days	(+/Y) La treatment alleviated the negative effect caused by induced drought stress in all concentrations. The best concentration was 11.11 mg L^{-1}
(SALEHI et al., 2018)	Ce, 203- 1628	*Phaseolus vulgaris*	Three-weeks old plants were sprayed with Ce suspension. 200 mL of nanoparticle suspension per treatment (n=3) were sprayed on leaves once every two days during two weeks	(-/N) Foliar application of CeO_2 nanoparticles caused alteration in stomatal density and length, photosynthesis, electron transport chain machinery. Moreover, nanoparticles induced oxidative stress and damage in membrane. The majority of effects were dose-dependent.
(XIE et al., 2015)	Ce, 13-326	*Cyclocarya paliurus*	Two foliar applications of Ce solution with interval of 15 days. The volume of each application was 300.	(Hormetic effect/Y) Improved the relative growth, increased content of soluble protein and sugar in leaf of plant treated with 65 mg L^{-1} of cerium nitrate. Harmful effect was verified in concentration at 326 mg L^{-1}
(YANG et al., 2014)	La, 11.3	*Glycine max*	Thirty-five days old plants were treated with La solution until drops began to fall.	(+/N) La treatment alleviated the luminous stress caused by UV-B radiation and enhanced its recovery of soybean seedling.
(MA; REN; YAN, 2014)	La, 56 Ce, 49	*Brassica chinensis L*	Twenty 20 days old plants were treated for 8 days with foliar solution	(+/N) La and Ce treatment promoted yield increase of *Brassica chinensis* L. and enhanced content of vitamin C and soluble sugar.
(MAO et al., 2012)	Ce, 11	*Glycine max*	Seedlings were evenly sprayed on the leaves until drops began to fall.	(+/-/N) The treatment with Ce at 20 mg L^{-1} alleviated UVB-induced water stress, however, it also reduced the growth of the plant.
(HUANG; WANG; ZHOU, 2013)	La, 11	*Glycine max*	Thirty-five days old were treated with La solution until drops began to fall	(+/N) La treatment alleviated the harmful effects of assimilation of nitrate caused by UV-B radiation.
(GAO et al., 2012)	La, 19	*Nicotiana tabacum*	Seven days old seedlings were treated with foliar solution during 3 days	(+/Y) La treatment alleviated the harmful effects caused by mosaic virus on *Nicotiana tabacum* photosynthesis and growth.
(IPPOLITO et al., 2011)	La, 6.9-1389	*Lycopersicon esculentum*	Twenty days old seedlings were treated with La solutions.	(Hormetic effect/N) La treatment at 16 and 32 mg L^{-1} reduced concentration of malondialdehyde and reduced some redox metabolites. Concentration above 138.9 mg L^{-1} caused chlorosis in leaf and increase the cellular H_2O_2.

Table 2.1. Bibliographical survey … (continued)

(PENG; ZHOU, 2009c)	La, 11	*Glycine max*	Seedlings were treated once with La solution until drops began to fall	(+/N) La treatment affected the balance of endogenous hormones and improved the resistance of soybean seedlings to UV-B stress.
(PENG; ZHOU, 2009b)	La, 11	*Glycine max*	Seedlings were treated once with La solution until drops began to fall	(+/N) La treatment reduced damage in chloroplast structure caused by UV-B stress.
(PENG; ZHOU, 2009a)	La, 11	*Glycine max*	Seedlings were treated once with La solution until drops began to fall	(+/N) La treatment increased the content of flavonoids in plant under UV-B stress indicating that La in suitable concentration can enhance the resistance of soybean plant against UV-B radiation
(LIU et al., 2007)	La, 69 Ce,2.8 Nd,72	*Spinacia oleracea*	Seeds were soaked in REE solution and at their four leaves stage their leaves were sprayed with same solution	(+/N) The ETRs improve in light energy transfer form PSI to PSII, photolysis and oxygen evolution
(XIAOQING et al., 2007)	Ce, 0.7- 4.2	*Spinacia oleracea*	Seeds were soaked in REE solution and at their four leaves stage their leaves were sprayed with same solution	(+/N) The Ce treatment at 1.4 mg L^{-1} improved the absorbance of visible light and the transference of energy among amino acids in PS II protein-pigment complex, besides that, increased the speed of energy transport from tyrosine residue to chlorophyll-a.

(+) Positive effect; (-) Harmful effect; (Y) Show biometrics data with difference statistical; (N) Biometric data neither presented statistical difference nor disclosed the biometric data

2.2 Materials and Methods

2.2.1 Preparation of La and Ce solutions for foliar application

La and Ce solutions at 200 and 2,000 mg L^{-1} were prepared from the $La(NO_3)_3.6H_2O$ P.A. and $Ce(NO_3)_3.6H_2O$ P.A. (VETEC, Brazil), respectively. The hydrocarbon based high wetting surfactant triton HW-1000 (The Dow Chemical Company, USA) was added in all treatments at 0.01% (v/v). Table 2.2 shows the composition of the two levels La and Ce solution treatments. Two controls were prepared: (a) deionized water containing the triton HW-1000 (WT 5) and (b) only deionized water (W6).

Table 2.2 Composition of La and Ce solution treatments utilized for foliar application

Treatment	Active	Concentration (mg L^{-1})	Surfactant triton HW1000 (%) (w/w)
La 1	La	200	0.01
La 2	La	2000	0.01
Ce 3	Ce	200	0.01
Ce 4	Ce	2000	0.01
WT 5	only water	-	0.01
W6	only water	-	-

2.2.2 Physico- chemical characterization of La and Ce solutions

The composition of La and Ce solutions and the control W6 utilized for physical chemical characterization are shown in Table 2.3.

The contact angle of La and Ce solutions and the control W6 droplet were measured on two faces of soybean leaf using a goniometer (Ramé-hart Instrument Co., USA, 250) standard model. Five microliters were pipetted on the adaxial and abaxial faces of the leaves and the contact angle was measured by the "DROPimage Advanced" software (Figure 2.1(a-b)).

Table 2.3 Composition of La and Ce solution treatments utilized for characterization

Treatment	Active	Concentration (mg L^{-1})	Surfactant triton HW1000 (%) (w/w)
W6	-	-	-
La 2 + Triton	La	2000	0.01
La 2 -Triton	La	2000	-
Ce 4 + Triton	Ce	2000	0.01
Ce 4 -Triton	Ce	2000	-

Solution drying time was determined by pipetting 1, 3, 5, 8 and 10 µL of La and Ce solutions and the control W6 (Table 2.3) on adaxial face of the soybean leaf and, subsequently, pictures taken every 4 min until the drying (Figure 2.1 (c-d)). The pH was measured using the pHmeter (Tec-2 Tecnal Tec-2, Brazil).

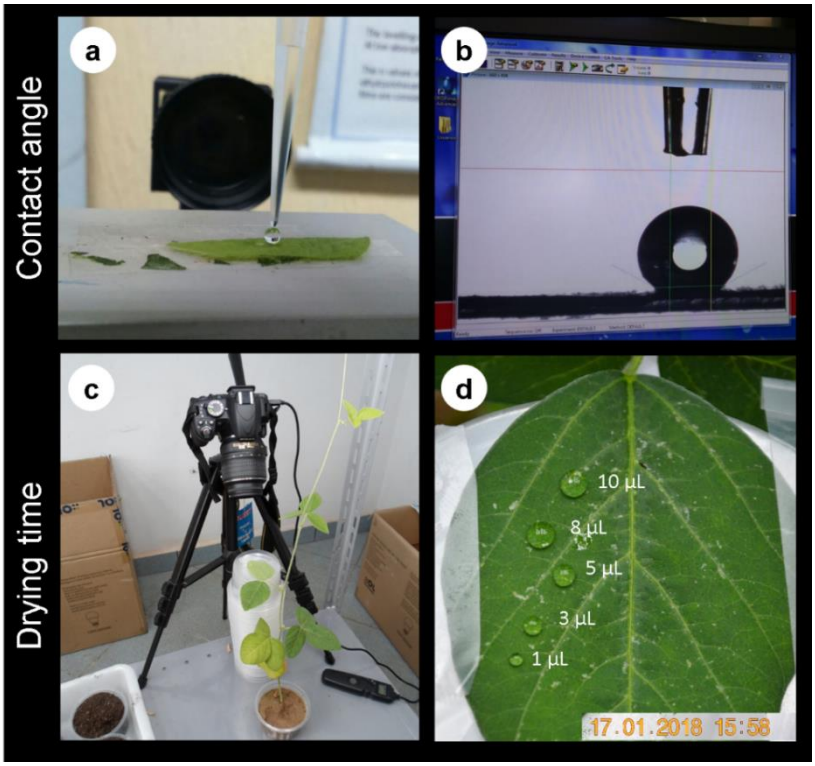

Figure 2.1 Instrumental arrangement used by to measure contact angle (a-b) and drying time (c-d). (a) droplet being deposited above soybean leaf cut in half. (b) picture used for to measure contact angle by the "DROPimage Advanced" software. (c) camera taking picture sequential every 4 min until the drop drying. (d) droplet pipetted with different volume above soybean leaf to calculate the drying time in function of volume.

2.2.3 Soybean cultivation

The soybean plants (RK7214 IPRO variety) plants were cultivated in a 3 L plastic pots, internally covered with plastic bag, containing sandy soil. They were cultivated in growth chamber at 27± 3 °C, 12 h photoperiod illuminated by LED lamps at a photon lux of 250 µ mol photons s^{-1} m^{-2}. Five soybean seeds were sowed in each pot. After the emergence, only the two healthier plants were left in the pot. Then, the plants were watered alternately with a 50 % Hoagland solution (HS) (HOAGLAND; ARNON, 1950) and deionized water every two days. The HS was prepared from pure grade reagents, in order to avoid REEs contamination. Then, when the plants reached the V4 stage (26 days old), we sprayed 0.5 mL of each corresponding treatment (a) $La(NO_3)_3$ $6H_2O$ and (b) $Ce(NO_3)_3$ $6H_2O$ solution at 200 and 2,000 mg L^{-1}, using the surfactant triton HW-1000 treatments at 0.01% (v/v) on adaxial leaf surfaces. This assay was carried out using five biological repetitions. During the spraying, the surface of the pot was fully covered with soft paper to avoid the soil contamination by La and Ce. The plants were cultivated until reaching the complete physiological maturity (83 days of experiment). The biometric data namely height of plants, number of leaves, relative chlorophyll content, number of pods and seeds per pods, and mass of seeds per treatment were weekly measured.

2.2.4 Lanthanum and cerium quantification in grains

The grains of the five repetitions were harvested, dried until constant weight, ground and digested in a laboratory microwave oven. The soybean grains were dried in an oven at 60°C and ground. Afterwards, an amount 0.2g were accurately weight into a pre-cleaned Teflon TFM tube, followed by the addition of 5.0 mL of sub boiling HNO3 20% (v/v) and 3.0 mL of H_2O_2 30% (m/m) (MA et al., 2015; SUN et al., 2013). The Teflon TFM tube was placed in the microwave oven (Provecto Analítica, model DGT 100-Plus). The program digestion was performed on 46 min divided in 3 steps: first step with 7 min at power 400 W, second step performed on 30 min at 850 W and finally third step on 7 min at power 320 W. After cooling, the solution was diluted to 20 mL with ultrapure water and transferred into a Falcon tube. The accuracy of the microwave digestion procedures was assessed by measuring the La and Ce concentration values in blank solution, certificate reference material NIST SRM 1573a, NIST SRM 1547 and spiked sample (spiked with stock standard solutions at 1 µg kg^{-1} of La and Ce) following the same digestion conditions of samples.

Concentration of La and Ce were determined by inductively coupled plasma mass spectrometer (ICP-MS) X-Series 2 (Thermo Scientific, Germany), equipped with a Mira Mist® nebulizer (Burgener Research Inc, Canada) and Thermo spray chamber at 4 °C. The optimized operating parameters of ICP-MS are summarized in Table 2.4.

Table 2.4 ICP-MS operational conditions for La and Ce determination

Parameter	**ICP-MS**
RF power	1350 W
Plasma	13.10 L min^{-1}
Flow rate nebulizer gas	0.98 L min^{-1} (optimized for 2% CeO/Ce)
Flow rate auxiliary gas	0.80 L min^{-1}
Peristaltic pump rotation	10 rpm
Sweeps	100
Dwell time	10 ms
Isotopes	139 La, 140 Ce, 142 Ce
Internal standard monitored	115 In, 159 Tb

The instrument was set to run a blank and a standard check at every ten samples. The solution containing Bi, Ho, In, Li, Sc, Tb and Y (10 µg L^{-1}) was used as a calibration internal standard for REE. The precision and accuracy of the analytical procedures were evaluated through the analysis of in certificate reference material NIST SRM 1573a, NIST SRM 1547 and spiked sample (spiked with stock standard solutions at 1 µg kg^{-1} of La and Ce). The limit of detection (LOD) and limit of quantification (LOQ) were determined based on the measurements of the standard deviation of 10 blank solutions.

2.2.5 Scanning electron microscopy (SEM)

For this, we pipetted 3 µL of 200 and 2000 mg L^{-1} La and Ce solution on leaves. Then four days later, the leaves were collected and immersed in Karnovsky fixative solution (KARNOVSKY, 1965) for 48h. Right after, they were sequentially dehydrated by immersion in a 10, 20, 30, 40, 50, 60, 70, 80, 90% (v/v) ethanol solution for 30 min each. Subsequently, the samples were dehydrated in 100 % ethanol for 1 hour. The latter step was performed three times. Finally, the samples were dried at their critical point (LEICA CPD 300), glued on aluminum stubs and coated with carbon (Balzers Union MED 010). Then, the samples were

analyzed by SEM-EDX. Further, the stubs were gold coated (Bal-tec model SCD 050) and examined with SEM (Jeol JSM IT 300). For the ultrastructural analysis, the samples were observed by secondary electron detector. To observe La and Ce distribution we used backscattered electron detector and SEM equipped with Oxford Instruments EDX detector.

2.2.6 Microprobe X-ray fluorescence

For microprobe X-ray fluorescence, we pipetted 3 µL of 200 and 2000 mg L^{-1} La and Ce solution on leaves. Then four days later, the leaves were harvested. Line scans and 2D maps were recorded using an Orbis PC spectrometer (EDAX, USA). In this equipment X-rays were provided by a Rh anode operated at 30 kV and 900 µA. A 25 µm thick Al primary filter was used to improve the signal-to-noise ratio. The X-ray beam was focused on the sample surface using polycapillary optics that yielded an X-ray beam nearly 30 µm wide. The samples were analyzed in two periods on the 4^{th} and 14^{th} day after application. The lines scans and 2 D maps were recorded using of dwell time of 30 and 10 s, respectively. For the latter analysis system, a matrix of 32 x 25 pixels was selected.

The signal threshold was calculated as shown in Equation 1:

$$Threshold\ (cps) = 8.45 * \sqrt{\frac{\boldsymbol{BG_{(average)(cps)}}}{\boldsymbol{t(s)}}} \qquad (1)$$

where $BG_{(average)}$ (cps) is the average of background under the La or Ce Lα XRF peak of sixty-four points of line scan and t (s) is the dwell time per point.

2.2.7 X-ray absorption near edge structure (XANES)

XANES spectra were recorded over the damaged spot in soybean leaf treated with La and Ce solutions. For this, three drops containing 5 µL of La and Ce solution at 2000 mg L^{-1} were deposited on a soybean leaf four days before XANES analysis.

Three XANES spectra were acquired from fresh leaf tissue at two damaged spots of each leaf. Three spectra were merged and used for the linear combination fitting (LCF). To avoid radiation damage, the scan was performed 2 mm away from each other.

The following reference compounds were analyzed: dried droplets of Ce $(NO_3)_{3(aq)}$ and La $(NO_3)_{3(aq)}$ deposited on Kapton film (same solution applied on the leaves), cellulose pelletized hexahydrate $La(NO_3)_3$ and $Ce(NO_3)_3$ and CeO_2, and finally La_2O_3 deposited on membrane.

The XANES spectra were recorded between -100 and 250 eV across La and Ce L_3 edge at XAFS2 beamline of the Brazilian Synchrotron Light Laboratory (LNLS). The beamline was calibrated measuring the K edge of vanadium metal foil. The harmonics were rejected with 20% of detuning. A nearly 500 μm wide monochromatic beam was employed, the detection was carried out in fluorescence mode (15-element Germanium Solid State Detector). Reference compounds were measured in transmission mode. Data normalization and LCF were performed using Athena (RAVEL; NEWVILLE, 2005). The linear combination analysis was performed on normalized spectra from -10 to 50 eV.

2.2.8 Statistical analysis

All statistical analysis was carried out by one-way analysis of variance (ANOVA) plus Tukey and Q tests at 95% confidence interval.

2.3 Results and Discussion

2.3.1 Characterization of foliar solution

Leaf wettability is an important feature that influences the effectiveness of foliar supplied chemicals and fertilizers (HAGEDORN et al., 2017). It can be measured through the contact angle between the droplet and solid surface. According to the literature, angles between 90° and 150° indicate a hydrophobic surface, while those above of 150° are considered superhydrophobic. Hydrophilic surfaces show angles between 10° and 89°, while angles below 10° are considered superhydrophilic (DAMATO et al., 2017; HAGEDORN et al., 2017)**.**

La 2-Triton and Ce 4- triton treatments presented a slightly contact angles decrease compared to the W6 control. The treatment containing the Triton HW 1000 at 0.01% (v/v) (La 2 and Ce 4) significantly reduced the contact angle by *ca*. 40% on the adaxial face and 20% on the abaxial one compared to the control (Figure 2.2 (a)), due to fact Triton HW 1000 (non-ionic surfactant) lowered the solution surface tension and increase the wettability. The adaxial face was more impacted by the surfactant than the abaxial one.

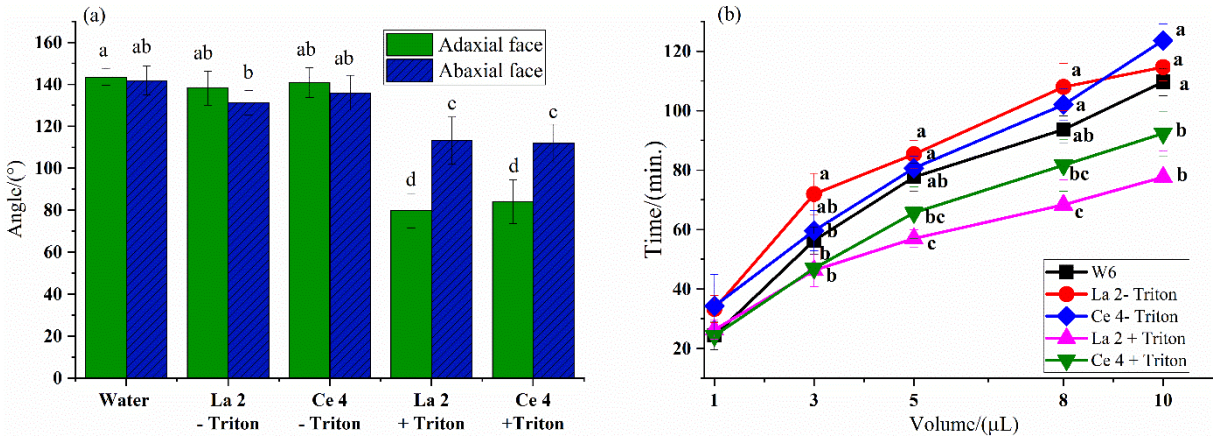

Figure 2.2. Contact angle (a) and drying time (b) of droplets of the La 2- Triton ($La(NO_3)_{3(aq)}$ at 2000 mg L^{-1}), Ce 4- Triton ($Ce(NO_3)_{3(aq)}$ at 2000 mg L^{-1}), La 2 ($La(NO_3)_{3(aq)}$ at 2000 µg L^{-1} + triton HW 1000 at 0.01% (v/v)), Ce 4 ($Ce(NO_3)_{3(aq)}$ at 2000 mg L^{-1}+ triton HW 1000 at 0.01% (v/v)) treatments and control (water) for the soybean leaf. The contact angle was measured in quintuplicate on adaxial and abaxial leaf face. The drying time were carried out in triplicate on adaxial face. Values followed by the same letter do not present statistical difference in Tukey test at 95% confidence level.

Our results show that the aqueous solution without surfactant did not show statistical difference between abaxial and adaxial leaf sides. The contact angle exhibited by deionized water (shown in Figure. 2.2 (a)) classify soybean leaf faces as a hydrophobic surface. Usually, the literature points out soybean leaf surface as a superhydrophobic or hydrophobic. This feature is attributed to the structure built above of the convex polygonal cells such as epicuticular wax crystals and trichomes (DAMATO et al., 2017; HAGEDORN et al., 2017).

Since the literature reports that the number of trichomes depends on the leaf face (BICKFORD, 2016), one could hypothesize that this factor influenced the contact angle. Nevertheless, the measured trichomes (Figure. 2.3) did not present statistical difference between the faces. Another possibility to explain the difference between faces regards possible differences in the morphology and chemical composition on adaxial and abaxial faces (BICKFORD, 2016).

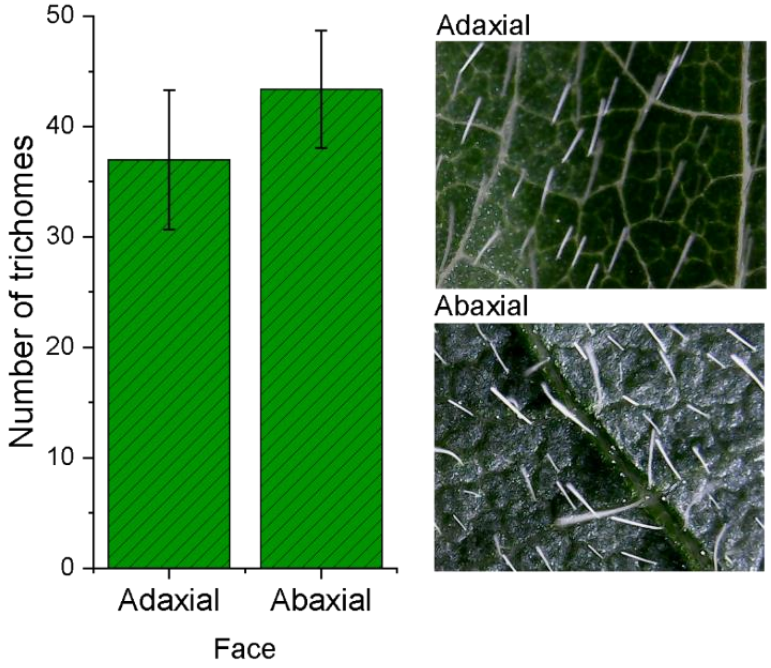

Figure 2.3. Trichrome density was measured on abaxial and adaxial face and we did not find statistical difference between the faces in Tukey test at 95% confidence level. The number of trichomes was measured in 3 leaves of 3 different plants summing up an of 9 different leaves

As a consequence of the smaller contact angle, the adjuvants also reduced the drying time of the droplets. This latter was also influenced by volume of droplet. The drying time presented in Figure 2.2 (b) was smaller for the solutions containing the surfactant which is caused by the larger surface area of the droplet. The time-volume relationship can be adjusted by the function described by Equation 2:

$$y = a * x^b \qquad (2)$$

where, y is the drying time, x is the droplet volume. The a and b coefficients can be adjusted and might be a function of physical chemical parameters of the solution and surface. Modeling studies will be addressed in future.

2.3.2 Effects of La and Ce on plant biometric parameters and La quantification in grains

The total mass of La and Ce supplied to each plant was ca. 1 and 0.1 mg for the higher (2000 mg L^{-1}) and lower dose (200 mg L^{-1}), respectively. Considering a population of 200 thousand plants per hectare and application of micronutrients such as Mn (350 g ha^{-1}) and

Zn (150 g ha^{-1}), the approximated mass of Mn and Zn supplied as foliar fertilizers per plant are 1.75 mg and 0.75mg, respectively (LACERDA et al., 2017; TEIXEIRA et al., 2004). Thus, the amount of La and Ce supplied to each plant intended to fall below (200 mg L^{-1}) and within (2000 mg L^{-1}) the concentration range of essential micro elements**.**

According to Figure 2.4 (a-h), the treatments did not affect the height of plants, number of leaves, relative chlorophyll content, number of pods and seeds per pods, and mass of seeds compared to the control under the Tukey test at 95 % confidence level.

The differences between the present study and those compiled in Table 2.1 might be related to the method of REE application, and their respective doses. In the present study, we applied 0.5 mL of foliar solution only once during complete cycle of soybean plant. Besides that, the high concentration applied on the leaves could trig the defense system of plants as a consequence of the salinity stress, that prevented great absorption of La and Ce, as it occurs to some micronutrients, for example B and Fe (FERNÁNDEZ; EBERT, 2005; WILL et al., 2011). Other possible disagreement concerns the statistical analysis, since not all studies reported the statistical analysis of the results.

Figure 2.5 shows that part of the La applied to the leaf surface was translocated to seeds. The concentration of La was higher in grains from plants treated with $La(NO_3)_{3(aq)}$ at 2000 mg L^{-1} than and 200 mg L^{-1}. LOD and LOQ of La was 0.04 and 0.1 µg kg^{-1}, respectively. Even though the content of La in the grains depended on the dose, the translocation rate was not linear. We can infer that only 3.2% of total applied was translocate from leaf to grains, in the first case ($La(NO_3)_{3(aq)}$ at 2000 mg L^{-1}), and 2.5% for second ($La(NO_3)_{3(aq)}$ at 200 mg L^{-1}). Due to the high level of signal obtained for blanks, it was not possible to accurately determine the transference of Ce from leaves to grains.

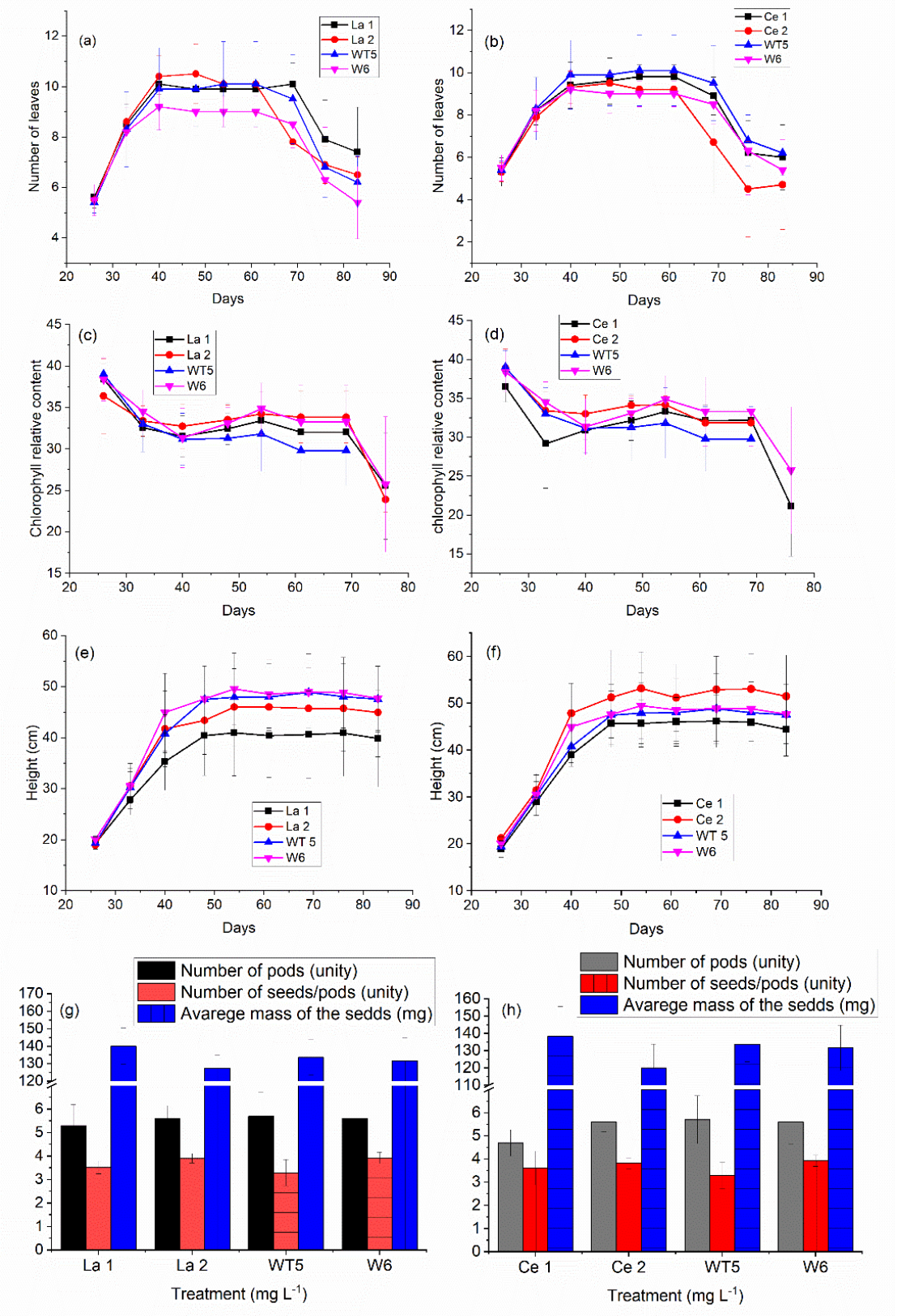

Figure 2.4. Biometric parameters of soybean: (a,b) height, (c,d) chlorophyll relative content, (e,f) number of leaves, and (g,h) number of pods, number of seeds per pods and average mass for La and Ce foliar application treatments. The measurements were carried out in quintuplicate. No statistical difference was found between both La and Ce treatments and the control at 95 % confidence level

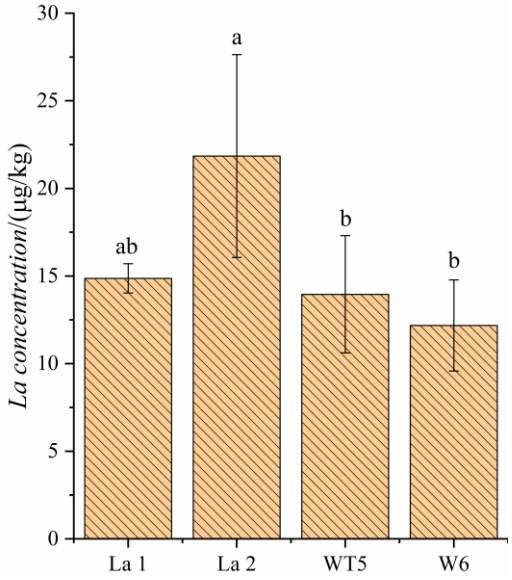

Figure 2.5. Lanthanum concentration in grains of soybean plants treated with La foliar solution. La concentration measurements were carried out using five biological repetitions. Same lower-case letters do not present statistical difference in Tukey test at 95% confidence level

2.3.3 Characterization of the lesions on the leaf surface

The soybean leaf is amphi-hypostomatic and covered by non-glandular trichomes. The epidermis is composed by a lens-shaped ordinary epidermal cells coated by epicuticular wax platelets. The deposition of Ce and La treatments culminated in the development of necrotic lesions surrounded by a chlorotic tissue. The presence of such lesions were noticed on the fourth day after the plants received the treatments. Figure.2.6 presents pictures of the lesions. These lesions may be resulted of a sequence of physiological, biochemical molecular steps that culminates with the cell death in the lesioned parts of the leaf. Harmful effects were shown in *Lycopersicon esculentum* when sprayed on leaves lanthanum at a concentration above 138.9 mg L^{-1} that caused chlorosis in and increase in cellular H_2O_2 (IPPOLITO et al., 2011). Similar injuries were found for *Vigna radiata* and *Zea mays* (DIATLOFF; ASHER; SMITH, 1999a) indicating that the high concentrations, approximately above 100 mg L^{-1}, were phytotoxic when sprayed on leaves. Likewise, harmful effects were shown in high concentration with other forms the exposure (SALEHI et al., 2018; MA et al., 2015; LIU; LIN; WANG, 2012; HU; WANG; WANG, 2006; TYLER, 2004).

The severity of the lesions was dose-dependent. Higher concentration caused larger necrosis area (Figure 2.6 (b;d)), while low concentration caused sparse small lesions (Figure 2.6 (a;c)). Despite these localized symptoms, as mentioned above, we did not observe any effects on biometric and production data between both treatments (Figure 2.4).

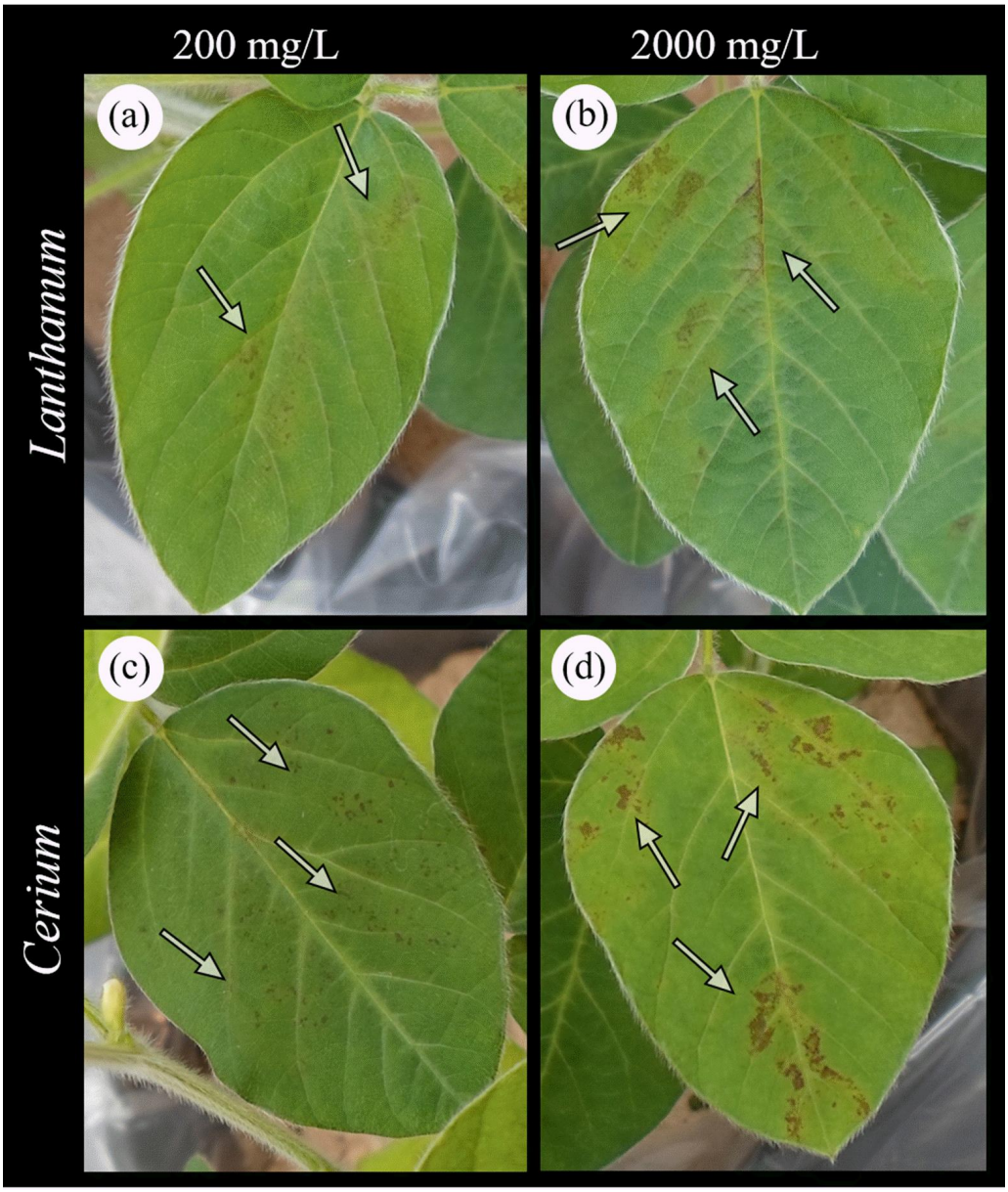

Figure 2.6. Pictures of leaves of *Glycine max* L. 7 days after La and Ce application. (a) 200 mg L^{-1} and (b) 2000 mg L^{-1} of lanthanum (c) 200 mg L^{-1} and 2000 mg L^{-1} of cerium. The arrows indicate the necrotic areas

Anatomical changes were noticed in leaves exposed to different doses of La and Ce (Figure 2.7). The adaxial soybean leaf surface presented outer periclinal wall epidermal cells covered with wax crystals (Figure 2.7 (a-c)). Although, the spray of La and Ce at dose of 200 mg L^{-1} did not cause large lesion on soybean leaf (Figure 2.7 (d-f and j-l)), it was observed cuticular changes in the tissue using the SEM high magnification. The wax crystals seem to be absent at the La and Ce deposition site. In addition, a collapse of the outer periclinal cell wall was also observed. The dose of 2000 mg L^{-1} caused drastic changes in leaf topography (Figure 2.7 (g-i and m-o)). It was also observed that, at low magnification, the lesioned regions are distinct comparing to neighbor tissues (Figure 2.7 (g and m)). At this dose, the epidermis presented collapsed cells with their losses related to the epicuticular wax crystals (Figure 2.7 (h-i and n-o)). Moreover, at the border of the lesion there is a gradient of collapsed cells. The mentioned degradation of the cuticle wax platelets is described in plants exposed to acid rain (ADAMS; CAPORN; HUTCHINSON, 1990), salinity, cold and pollution (SHEPHERD; WYNNE GRIFFITHS, 2006). A similar effect was observed in soybean leaves exposed to high dose 300 mmol L^{-1} of Mn (SANTOS et al., 2017). Altogether, the SEM results showed that application of cerium and lanthanum solutions seems to be harmful to the soybean leaf structure at the doses used in the present study.

The µ-XRF was used to verify the correlation between the damaged spot the presence of La and Ce (Figure 2.8). The signal threshold was 8.5 cps for La and 10.6 cps for Ce. Figure 2.8 shows a positive spatial correlation between the scorching and the presence of La (Figure 2.8(a-d)) and Ce (Figure 2.8 (e-h)). In addition, for both REE treatments it was possible to note a damage gradient, in which the chlorotic damages (yellowish color) presented smaller content of the corresponding REE, while at necrotic damage area (brownish color) higher the REE presence was found. The pictures showed that Ce treatment was more aggressive than La, even though they were at the same concentration (Figure 2.8 (e-h)). Diatloff et al. (2008) presented that similar effect in corn and mungbean. One hypothesis that may explain these results is the chemical physical difference that these two elements present, such as the oxidation state. Where La presents only oxidation state +3 the Ce can presents two +3 and +4 (HAYNES, 2014), likewise micronutrients Fe (FERNÁNDEZ; EBERT, 2005).

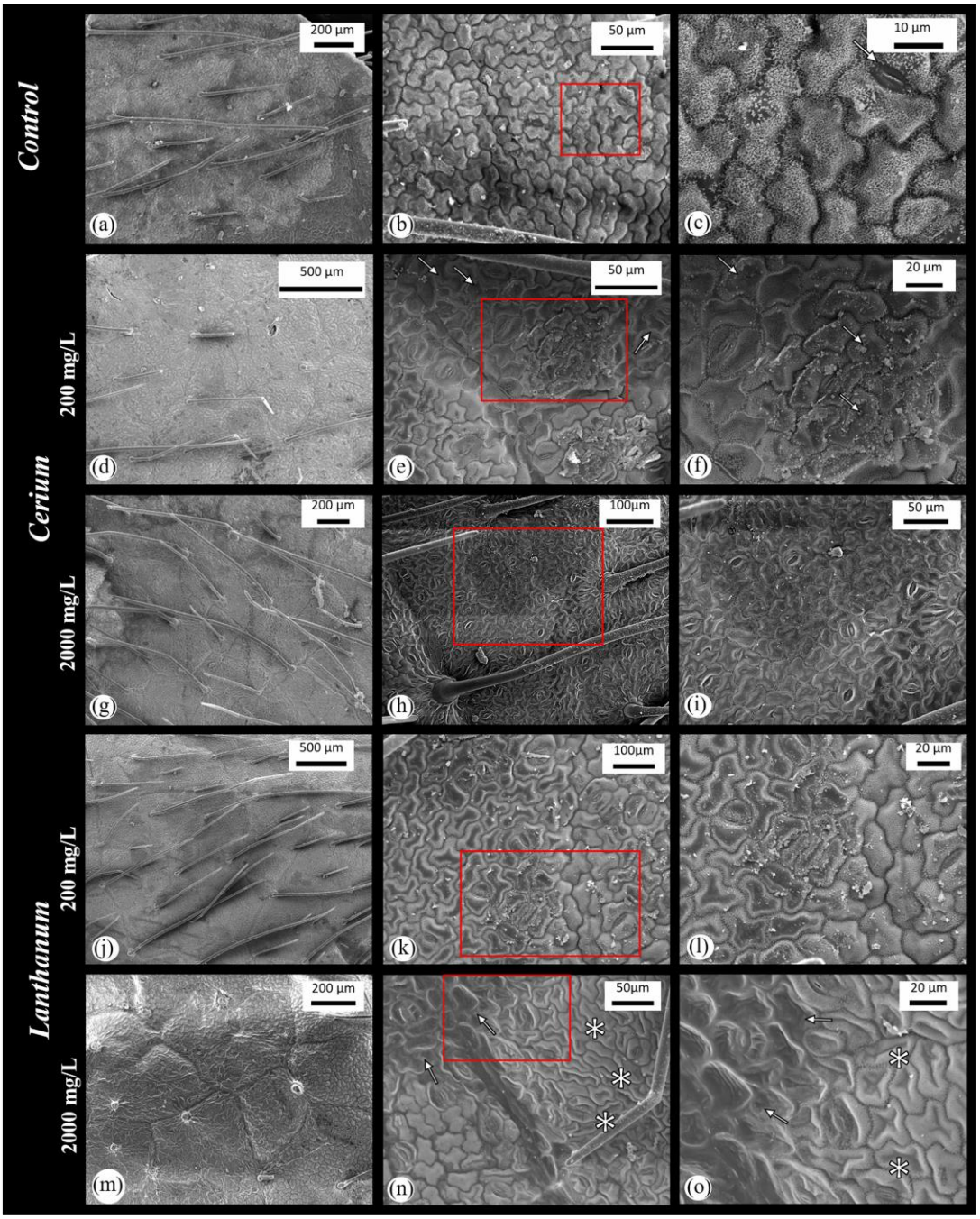

Figure 2.7. Electron-micrographs gold-coated of the adaxial surface of *Glycine max* L. leaves. Treatment with distilled water (a-c), different doses of cerium (d-i) and lanthanum (j-o). Overview of the leaf surface in a; d; g; j; and m. Detail of highlight with red square in c, f, i, l, and o. Arrows highlight stomata in c. Arrows indicating collapsed cells in e-f. Note scale gradient of necrosis and chlorosis indicated with arrow and star respectively in n and o.

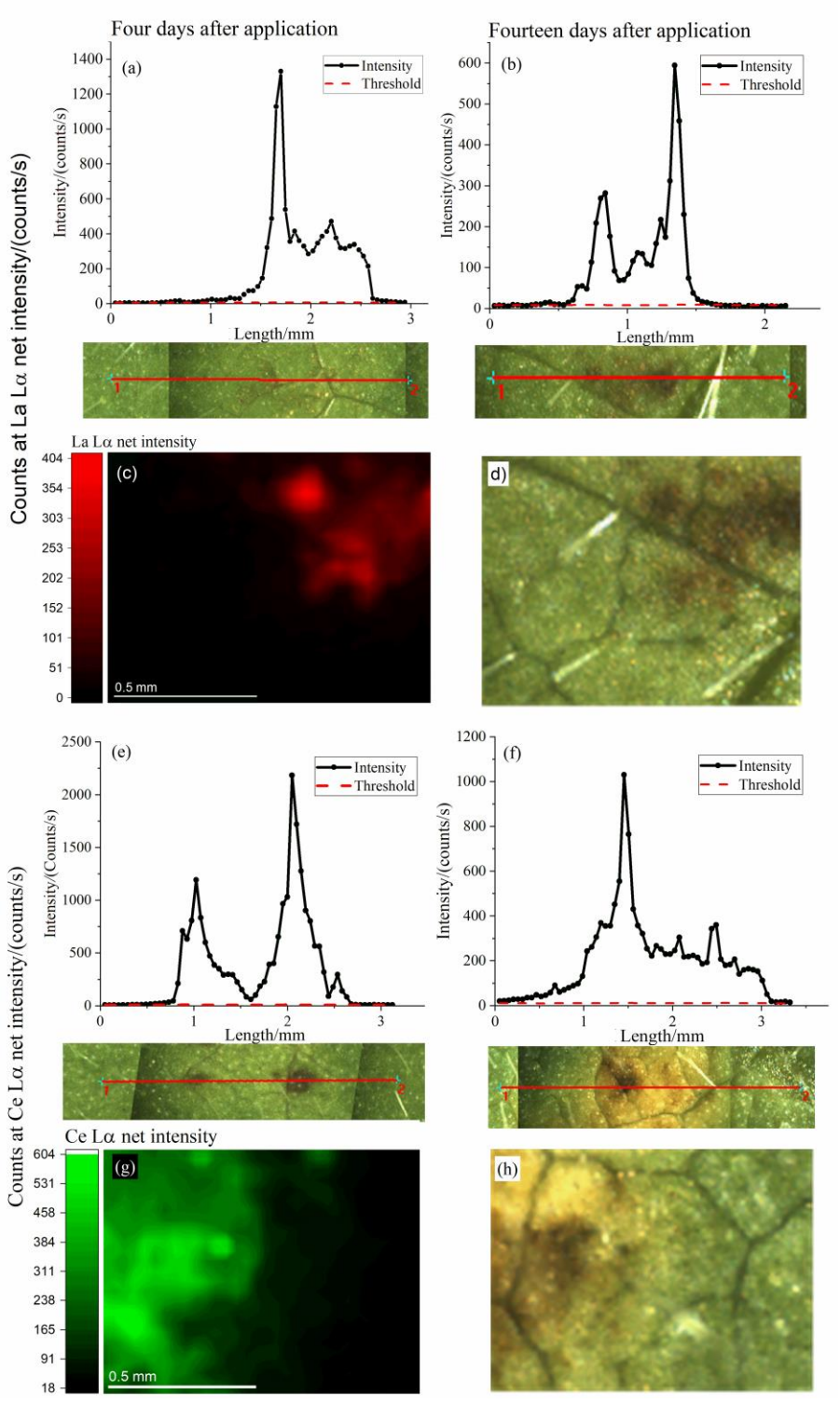

Figure 2.8. Microprobe X-ray fluorescence (μ-XRF) analysis on the adaxial surface of *Glycine max* L. La-Lα line scan along the leaf damage (a) 4 days after application of La at 2000 mg L^{-1} and (b) after 14 days. (c) La distribution and (d) the optical image of the damage area after 14 days of foliar application. Ce-Lα line scan along the leaf damage (e) 4 days after application of Ce at 2000 mg L^{-1} and (f) after 14 days. (g) Ce distribution and (h) the optical image of the damage area after 14 days of foliar application. Below of each the La and Ce line scan graphs, their corresponding optical images are shown, in which a red line indicate the line scanned.

The LCF allows comparing the XANES spectra of samples and standards and determine the chemical environment of La and Ce deposited at the leaf. LCF obtained for spectra recorded at the damages caused by La treatment show a mixture of 48% $La(NO_3)_3$ and 52% La_2O_3. At the lesions caused by Ce, the spectra were fitted as 63% of $Ce(NO_3)_3$, 19% $Ce(NO_3)_3$ + triton and 18% of Ce oxide (Figure 2.9(a-d)).

The presence of oxides at the lesions show that the pristine nitrates were bio transformed by the plant. The bio transformation of the La and Ce nitrate to oxide form may be result of cell degradation caused by high concentration of REE, characterized as burning of leaves after foliar application (FAGERIA et al., 2009). The chemical reaction might depend on the initial state of the applied REE since other studies employing CeO_2 detected root-to-shoot transported, but did not observe chemical transformation of CeO_2 (LÓPEZ-MORENO et al., 2010).

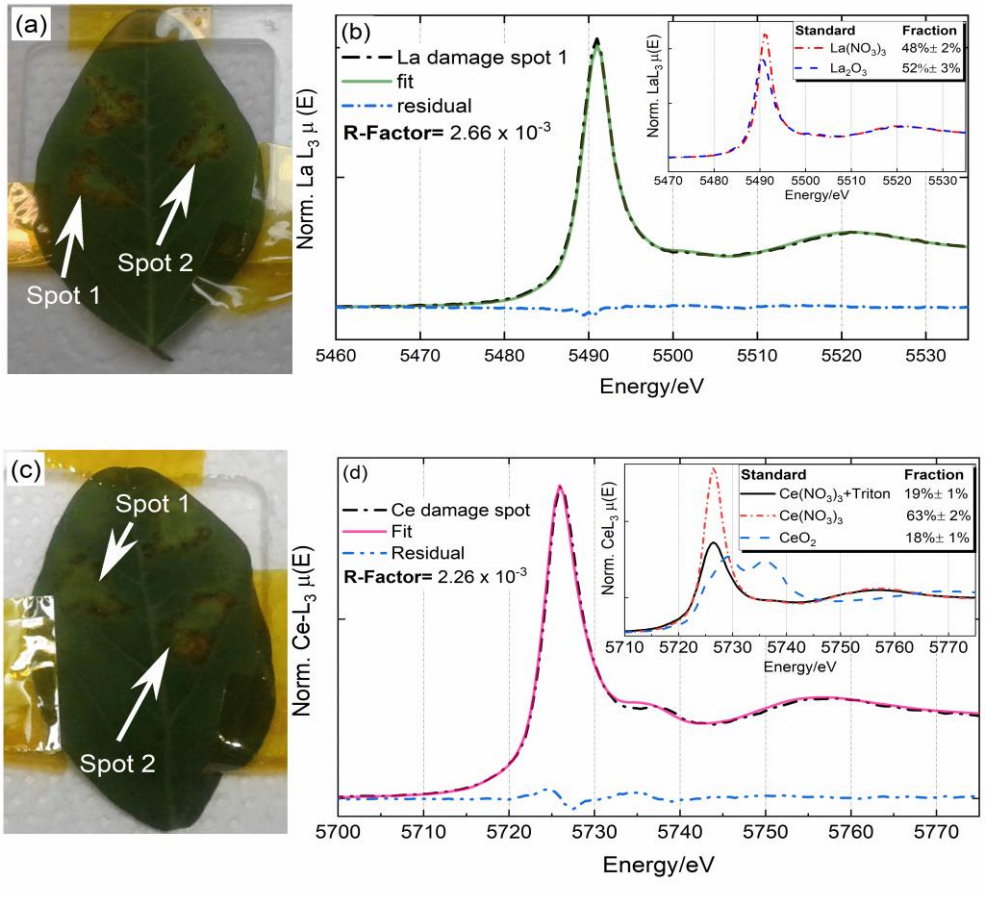

Figure 2.9. Linear combination fit (LCF) for La L_3 and Ce L_3 edge XAS spectra recorded. Pictures of leaves showing three spot damage caused by foliar application of $La(NO_3)_{3(aq)}$ at 2000 mg L^{-1} concentration (a) and Ce $(NO_3)_{3(aq)}$ at 2000 mg L^{-1} concentration (c). The overlap of LCF with the average spectra of La spot 1 leaf 1 fitted as a mixture of $La(NO_3)_3$. $6H_2O$ pellet and La_2O_3 membrane (b). The overlap of LCF with the average spectra of Ce spot 1 leaf 1 fitted as a mixture of Ce $(NO_3)_3$. $6H_2O$ pellet and Ce_2O_3 membrane and $Ce(NO_3)_3$ plus triton. The analysis was carried out in two damage spot and the average spectra of each damage spot was obtained through three spectra. All analysis data were performed in software Athena.

2.4 Conclusions

Altogether, the study showed that the addition of Triton 0.01% (v/v) improved the wettability of aqueous solutions of Ce and La nitrates. The adaxial face was more sensitive to the presence of the surfactant, however it cannot be attribute to the number of trichomes on this leaf face.

Even though we found evidence of REE absorption and transport from leaves to grains, the application of La and Ce at 200 and 2000 mg L^{-1} did not affect the soybean plant biometrics (plant height, number of leaves and relative chlorophyll content) and grain yield (number of pods and seeds per pods, and mass of seeds per treatment).

The foliar treatments induced the appearance of leaf damages such as chlorosis and necrosis. The La and Ce nitrates deposited on the leaf surface were partially bio transformed into oxides; such reactions might be responsible for the lesions.

The lesions were associated to the hotspots of Ce and La, from the microscopic standpoint it was observed alteration on the epicuticular wax and collapse of the outer periclinal cells. Cerium treatment was more harmful than La at both concentrations.

To achieve possible beneficial effects on soybean production parameters, further studies must be conducted under lower concentration of Ce and La. Additionally, the dose should be divided in multiple applications.

3 EFFECT OF NANO CERIUM OXIDE ON SOYBEAN (*GLYCINE MAX* L. MERRILL) CROP: A PERSPECTIVE TOWARDS ITS 2050'S CONCENTRATIONS

Abstract

Cerium (Ce) is one of the rare earth elements (REE) that has received special attention in the last two decades due to its different industrial applications, many of which use nanoparticle. Consequently, the intense use of Ce nanoparticles (NPs) and their subsequent fate and accumulation in the environment has raised concerns about their toxicity. Within this horizon, we herein evaluated the absorption and translocation of CeO_2 NPs and soluble $Ce(NO_3)_3$, from root to shoot and from root to grains, by soybean (*Glycine max* L.) Merrill) plants. The applied concentrations were the same as those predicted to occur by the year 2050 in agricultural and sludge-treated soils (0.062 and 0.933 μg kg^{-1}, respectively). Microprobe X-ray Fluorescence spectroscopy (μ-XRF) and single-particle Inductively Coupled Plasma Mass Spectrometry (SP-ICP-MS) techniques were employed to detect and quantify Ce within soybean tissues. Cross section μ-XRF analysis of the soybean roots showed Ce on its internal tissue, revealing that these plants were able to take up Ce and translocate it to other plant tissues, as demonstrated by ICP-MS analysis of the shoot and grains of the soybean. However, plant development and yield were not affected by Ce exposure at any of the tested concentrations. In addition, kinetic study with $Ce(NO_3)_3$ treated plants showed that Ce translocation from root to shoot was time-dependent. On the other hand, no difference in uptake rate was found for CeO_2 NPs treatment over a period of four weeks. SP-ICP-MS analysis detected Ce NPs in the shoots of soybean with an average size higher than was applied (60.3 nm). All results presented here provide evidence that soybean can absorb and translocate Ce in the soluble and NPs forms from roots to shoot and grains, highlighting the concerns regarding the introduction of Ce NPs in the food chain.

Keywords: Single-particle ICP-MS; X-ray fluorescence spectroscopy; Rare earth elements; Soybean; CeO_2 nanoparticles

3.1 Introduction

In addition to soluble forms, there is an increasing interest on nanoparticles. The Nanotechnology Consumer Product Inventory shows an increase of *ca*.75% of products that used nanotechnology in period of 2010 to 2014 (VANCE et al., 2015).

Cerium oxide nanoparticles have received major attention within the last two decades due to its several industrial applications thanks to the oxygen storage capacity. It has been applied as automotive catalytic converters, fuel additive, polishes for glass and silicon wafers, and automotive NiMH-batteries (GIESE et al., 2018).

The increased use in the industry had reflected in the increase by nearly50% on the number of publications about Ce based nanoparticles (Ce NPs) in the Web of Science database between the 2014-2018 compared to 2009-2013. In view of these facts, the increase of concentration of Ce NPs in the environment is hardly questionable. Thus, a deeper investigation on the impact of these nanomaterials on plants must be carried out.

The intense use of Ce NPs raises the concern about its release in the environment and their potential harmful effects on living systems. Hence, GIESE et al., (2018) predicted concentrations of 0.062 and 0.93 mg kg^{-1} of Ce NPs (CeO_2) by 2050 in agricultural and sludge-treated soils, respectively. To perform the calculation, they took into account the estimative of NPs production volumes, application method, end-of-life, and also the mass released to the atmosphere, water, and soil (GIESE et al., 2018).

The Single Particle Inductively Coupled Plasma Mass Spectrometry (SP-ICP-MS) characterization technique is a suitable tool to study the interaction of nanoparticles and plants. This technique allows the simultaneous determination of concentration and size distribution of nanoparticles (DAN et al., 2016; TUORINIEMI; CORNELIS; HASSELLÖV, 2014). Several studies reported using SP-ICP-MS to found Ce NPs in the shoot of plants that received root treatment of Ce NPs, such as in *Raphanus sativu*s (L.) (WOJCIESZEK et al., 2019), *Cucumis sativus* L.(ZHANG et al., 2011; 2012), *Solanum lycopersicum* L, *Cucurbita pepo*, and *Glycine max* L. (DAN et al., 2016). These studies evidenced the ability of superior plants to uptake and translocate Ce NPs, although the majority of the applied Ce NPs remain adsorbed on the root surface, as demonstrated by Ma et al. (2015) using μ-XRF.

It seems that Ce NPs can induce harmful and/or beneficial effects, depending on the particle size, concentration, and plant species. According to the bibliographic survey presented in Table 3.1, these effects are usually related to alterations in the photosynthesis and enzymatic antioxidant system. It is important to highlight that toxicity is commonly reported to occur in concentrations from 100 to 3000 mg kg^{-1} or mg L^{-1} (Table 3.1), *ca.* 100-fold higher than the highest concentration predicted by 2050 (GIESE et al., 2018).

The literature have clearly demonstrated that nanoparticles can be taken up by plants (DAN et al., 2015; DA CRUZ et al., 2017; 2019; RAI et al., 2018). However, perhaps a pivotal question to be addressed is: Are the nanoparticles absorbed in their pristine form or they are dissolved, and the ions are actually taken up?

In this context, the present study aimed at investigating whether the concentration of Ce NPs predicted by 2050 affects soybean development and grain yield. Additionally, we verified whether cerium present in plant tissue was in nanoparticulate form. For this, the roots of soybean plants (*Glycine max* L.) were exposed to CeO_2 NPs and $Ce(NO_3)_3 \cdot 6H_2O$. We employed SP-ICP-MS and microprobe X-ray fluorescence spectroscopy (μ-XRF) techniques to locate, characterize and quantify Ce in plant tissues and verify the ability of soybean to take up and translocation Ce from root to shoot and grains. Finally, SP-ICP-MS was employed to determine cerium chemical species.

Table 3.1 Bibliographical survey on the effect of NPs Ce on plants. The studies presented herein were 20 newest publications dealing with root application of cerium based nanoparticle. This survey was carried out at the Web of Science research platform with the keywords: “nanoparticle”, “cerium” and “uptake” on August 14th 2019

Reference	CeO_2 Concentrations	Size (nm)	Substrate	Plant species	Main effects
(HAMIDREZA; XIAOXUAN; XINGMAO, 2019)	100 mg L^{-1}	30-50	nutrient solution	*Glycine max* L. (soybean)	Did not affect plant growth
(WOJCIESZEK et al., 2019)	5 mg L^{-1}	30-50	nutrient solution	*Raphanus sativus* L. (radish)	Did not affect plant growth
(SALEHI et al., 2018)	0;250; 500; 1000; 2000 mg L^{-1}	10-30	soil	*Phaseolus vulgaris* L. (bean)	(-) Harmful effect in the morphological, biochemical, proteomic and metabolomic assay
(YANG et al., 2017)	100; 200; 500; 1000; 2000; 3000 mg L^{-1}	10-15	petri dishes with agar medium	*Arabidopsis thaliana* L..	(-) Decrease on growth, photosynthetic and antioxidant systems at 1000-3000 mg L^{-1}.
(CAO et al., 2017)	0; 10; 100; 500 mg kg^{-1}	10-30	soil	*Glycine max* L. (soybean)	(+/-) Increase in plant growth and photosynthetic rate at 100 mg kg^{-1}. Reduction of net photosynthetic rate (36%) at 500 mg kg^{-1}
(GUI et al., 2017)	0; 10; 50; 100 mg kg^{-1}	<25	soil	*Raphanus sativus* (radish)	(+) Increase fresh biomass, chlorophyll content affected and enzyme activity
(SERVIN et al., 2017)	0; 500; 1000; 2000 mg kg^{-1}	20-200	soil	*Lactuca sativa L* (lettuce); *Cucurbita pepo L*(Zucchini); *Glycine max* L. (soybean); *Zea mays L.*(corn)	(-) Increase lipid peroxidation and decrease in content of chlorophyll a, b and carotenoid in all treatments
(MAJUMDAR et al., 2016)	62.5; 125; 250; 500 mg kg^{-1}	~8	soil	*Phaseolus vulgaris* L. (kidney bean)	(+/-) At 62.5-250 mg kg^{-1} enhance transpiration rate and stomatal conductance, on the other hand decrease in the carotenoid content.

Table 3.1 Bibliographical survey... (continued)

(DU et al., 2015)	100; 400 mg kg^{-1}	8±1	soil	*Triticum aestivum* L. (wheat)	(-) Decrease in chlorophyll content and increase of catalase and superoxide dismutase activities at 400 mg kg^{-1}.
(GUI et al., 2015)	50; 100; 1000 mg kg^{-1}	< 25	soil	*Lactuca sativa* (lettuce)	(+/-) Faster grow and increasing on nitrate content at 100 mg L^{-1}; Interruption of stress response activity (Superoxide dismutase (SOD), Peroxidase (POD), and Malondialdehyde(MDA) at 1000 mg kg^{-1}
(NHAN et al., 2015)	100; 500 mg L^{-1}	10±3.2	nutrient solution	*Bacillus thuring- iensis* (Bt)-transgenic cotton	(-) Damage of chloroplasts and decreasing of Zn, Mg, Fe and P content in the xylem.
(RICO; PERALTA-VIDEA; GARDEA-TORRESDEYA, 2015)	62.5; 125; 250; 500 mg L^{-1}	8±1	petri dishes with agar medium	*Oryza sativa L. (rice*), *Triticum aestivum* L. (wheat)	(-) Harmful modification on the root xylem composition of all sampled plant species.
(MAJUMDAR et al., 2014)	10 mg L^{-1}	10-30	nutrient solution	*Raphanus sativus* L. (radish)	Did not affect plant growth
(RICO et al., 2014)	125; 250; 500 mg kg^{-1}	8±1	soil	*Triticum aestivum* L. (Wheat)	(+/-) Increase in plant growth, shoot biomass, and grain yield; Decreasing of S and Mn storage in the grains for all treatments. Modification of amino acid composition and linoleic acid in grais at 125 mg kg^{-1}. Increase in grain proteins
(CUI et al., 2014)	2; 20; 200; 500; 1000; 2000 mg L^{-1}	7.1±0.4	petri dishes with agar medium	*Lactuca sativa Linn. var. angustata Irish ex Bremer (*asparagus lettuce)	(-) Inhibition of root growth and modification of superoxide dismutase activity, induction of lipid peroxidation and damage of cell membranes at ≥500 mg L^{-1}
(MAJUMDAR et al., 2014)	62.5; 125; 250; 500 mg L^{-1}	8±1	nutrient solution	*Phaseolus vulgaris* L. (kidney bean)	(-) Decrease of root enzymatic activity at 500 mg L^{-1}
(SCHWABE et al., 2013)	100 mg L^{-1}	17-100	nutrient solution	*Triticum aestivum* L. (Wheat); Cucurbita maxima (pumpkin)	Did not affect plant growth

Table 3.1 Bibliographical survey... (continued)

(MORALES et al., 2013)	62.5; 125; 250; 500 mg kg^{-1}	8±1	soil	*Coriandrum sativum* (.)L (Cilantro).)	(-) Increase on catalase activity at 125 mg kg^{-1}; Biomass reduction at 250 mg kg^{-1}
(RICO et al., 2013)	500 mg kg^{-1}	8±1	soil	*Oryza sativa*L. (rice)	(-) Decrease of Fe, S, prolamin, gluten, starch, lauric and valeric acids, and antioxidants (except flavonoids)
(MA et al., 2013)	250; 500; 1000; 2000 mg L^{-1}	10-30	petri dishes with agar medium	*Arabidopsis thaliana* L.	(-) Decrease of chlorophyll production (60-85%). Modification of the stress response gene expression (e.g. glutathione [GSH])
(LÓPEZ-MORENO et al., 2010)	500; 1000; 2000; 4000 mg L^{-1}	7	petri dishes with filter paper	*Medicago sativa* (alfalfa); *Zea mays* (corn); *Cucumis sativus* (cucumber); *Lycopersicon esculentum* (tomato)	(-) Decreasing of germination rate (20-30%) at 2000 mg L^{-1}

(+) positive effect; (-) harmful effect

3.2 Material and Methods

3.2.1 Reagents and instruments

Cerium oxide (CeO_2) NPs was purchased from MKnano (99.9 %, Canada) with an average size of 25 nm, as informed by the supplier, while Ce (III) nitrate hexahydrate ($Ce(NO_3)_3 \cdot 6H_2O$) was purchased from Sigma-Aldrich (99% grade, USA). Both were used to prepare 303 mg L^{-1} primary dispersions and solutions of Ce. Stock Ce solution at 1000 mg L^{-1} (Sigma-Aldrich, USA) was used to prepare the calibration curve and spike testing. The nitric acid (65 %, grade) and hydrogen peroxide (30 %, certificate grate ACS) used in microwave sample digestion were obtained from Fisher Chemical (USA). For enzymatic digestion, Macerozyme R-1^{-}0 enzyme (Pectinase from *Rhizopus* sp, bioWORLD, USA) and citrate buffer 0.09 M (pH 4) from Sigma-Aldrich (USA) were used. Ultrapure water at 18.2 M Ω cm^{-1} was used in all experimental steps. All salts employed in the hydroponic solution were laboratory grade.

Cerium NPs were dispersed in water using an ultrasonic processor (Sonics, vibra-cell ultrasonic liquid processor, USA). All samples were digested in a laboratory microwave oven (PerkinElmer Titan MPS, USA). A shaker incubator (VWR Floor, Shaking Incubator -1585, USA) was employed for the enzymatic digestion. An inductively coupled plasma mass spectrometer (Perkin Elmer, NexION 2000 ICP Mass Spectrometer- PerkinElmer) was used to measure both nanoparticle and dissolved Ce. The line scan was measured by Orbis PC spectrometer (EDAX, USA).

3.2.2 Soybean cultivation

Soybean cultivation in the growth chamber

Soybean seeds (*cv.* Monsoy 7739 IPRO) were sown in sandy soil until reaching the V2 phenological stage. Afterwards, the plants were transferred to 2 L plastic pots containing a hydroponic solution (CAKMAK; MARSCHNER, 1988). Seven days after, (plants at V3 phenological stage), CeO_2 NPs dispersions and $Ce(NO_3)_3$ solutions were spiked in nutrient solution at 0.05 and 0.75 mg L^{-1}. For the sake of information, these concentrations, expressed in mg L^{-1}, refers to the elemental Ce levels, not the Ce compound. The control treatment followed the same conditions, except the Ce addition. The nutrient solution was weekly

replaced. The experiment was conducted in a growth chamber at 27°C with 12 h photoperiod illuminated by LED lamps at a photon flux of 250 μmol photons s^{-1} m^{-2}.

The experiment was carried out with 10 biological replicates for each treatment and divided into two steps. In the first one, five plants of each treatment were harvested after two weeks of Ce exposure, and then the Ce concentration in the shoot was measured. In the second step, the soybean plants were cultivated until their final stage (R8 phenological stage) to verify if Ce was translocated to the grains.

Plant height, number of leaves and relative chlorophyll content were weekly measured. At the end of the experiment (115-days-old plants), the number of pods and seeds per pods, and the total mass of seeds of each treatment were determined.

Soybean cultivation in greenhouse

Similarly, to the growth chamber cultivation procedure, the soybean plants were also grown in a greenhouse (ca. 37°C). For this latter assay, the plants were transplanted to hydroponic solution (CAKMAK; MARSCHNER, 1988) 10 days after germination. Then, after one-week (V3 phenological stage) Ce was spiked as 25 nm CeO_2 NPs and Ce $(NO_3)_3$ at 0.75 mg L^{-1} of Ce. A kinetic study was conducted after the Ce spiking for four weeks, five plants of each treatment were weekly collected and the Ce concentration in the leaves was determined by ICP-MS.

3.2.3 μ-XRF

After the soybean grain harvest, the root apex of each treatment was excised and cross sectioned (ca. 1 mm thick). This slice was placed on a XRF sample holder and analyzed by μ-XRF (RODRIGUES et al., 2018). The equipment operating conditions are described in Table 3.2. The analysis was performed with three biological replicates of each treatment.

Table 3.2 Operation conditions µ-XRF

Current	900 µA
Tension	30 kV
Primary filter	Al 25 µm
Time per point	30s
Bean size	30 µm

3.2.4 Sample preparation for ICP-MS and Single Particle ICP-MS

Acidic digestion

Soybean shoots and grains (dried in lab oven at 60° and ground in mill machine) were weighed (ca. 0.4 g) and transferred to 70 mL Teflon^{TM} digestion tube. Then, 4 mL of nitric acid (60%) and 3 mL of hydrogen peroxide (30 %) were added to the digestion tubes. The tubes were closed and digested by a laboratory microwave oven following the operating conditions shown in Table 3.3.

Table 3.3 Program to be used in microwave acid digestion

Step	**Time (min)**	**Power (w)**
1	7	400
2	15	850
3	7	320
4	2	0

After the digestion procedure, the teflon tubes were cooled down to room temperature, and the digested samples were transferred to 50 mL volumetric flasks and made up to 50 mL with ultrapure water. Before the ICP-MS analysis, the samples were diluted 10-fold.

Enzymatic digestion

After kinetic evaluation, soybean leaves were harvested and cut in small pieces using a scissor, and then ground in liquid nitrogen and stored in a freezer (-18 °C). For enzymatic digestion, ground soybean shoot samples (*ca.* 0.1 g) were transferred to a plastic vial containing

9 mL of citrate buffer 0.09 M (pH 4). Afterwards, 1 mL of Macerozyme R-10 enzyme at 30 mg mL^{-1} was added. The sample was digested at 37 °C for 48 h in a shaker incubator at 230 rpm.

Right after the sample digestion, the samples were left at rest for ca. 1 h. Then, an aliquot of 0.1 mL of the supernatant was taken and diluted 100-fold using ultrapure water. Subsequently, the samples were filtered using a Millipore 5 kDa Ultrafree®-MC. Finally, the filtered samples were analyzed by SP-ICP-MS.

3.2.5 ICP-MS and SP-ICP-MS analysis

^{140}Ce was chosen to be monitored since it is the most abundant Ce isotope (88.45%) and it does not present any interference (DAN et al., 2016). The ICP-MS operating conditions are shown in Table 3.4. The analysis was performed with five biological replicates of each treatment and five analytical replicates. The trueness of the ICP-MS method was verified by spiking $Ce^{3+}_{(aq)}$ at 0.1, 0.5 and 1 ug L^{-1} in the control sample before the acid digestion.

Table 3.4 Optimized ICP-MS operating condition

Parameters	**Values**
Nebulizer gas flow, L/min	1.02
Plasma gas flow, L/min	15
ICP RF power	1600
Analog stage voltage	-1675
Pulse stage voltage	1100
Cell entrance voltage	-4
Cell exit voltage	-4
Cell rod offset Sampler cones	-17
SP-ICP-MS method parameters	
Analyte	^{140}Ce
Mass (amu)	139.905
Dwell time, ms	50
Mass fraction, %	81.39
Density, g/cm^3	7.13
Ionization efficiency, % a	100
Transport efficiency, %	5.26
Sample flow rate ml/min	0.48

The accumulation value was calculated considering the Ce concentration and total mass of shoot and grain of each biological replicate.

The SP-ICP-MS operating conditions for determining CeO_2 nanoparticle are shown in Table 3.4. The transport efficiency was calculated based on the particle concentration. For this, a standard dispersion of 50 nm spherical gold nanoparticle at 100,000 nps mL^{-1} (nanoparticles/mL) was used for equipment calibration, in which was measured the ^{196}Au isotope.

Some researchers have reported that plants are able to partially biotransform CeO_2 NPs in cerium carboxylate and cerium phosphate (LÓPEZ-MORENO et al., 2010; ZHANG et al., 2012), however, pristine CeO_2 is the predominant form (ZHANG et al., 2012). Therefore, herein we considered that all signal obtained was of the compound CeO_2. The effect of the sample preparation (cryogenic grinding and enzyme solution adding) on Ce NPs were verified by spiking Ce NPs dispersion at 7 ug L^{-1} in the control sample just before the grinding and after enzymatic digestion steps.

3.3 Results and Discussion

Both Ce concentrations (0.05 and 0.75 mg L^{-1}) used in this experiment were based on the estimated upper limits of CeO_2 NPs 0.062 and 0.93 mg kg^{-1} of CeO_2, respectively. These figures may be found in agricultural and sludge treated soils, respectively, by 2050 (GIESE et al., 2018). This report considered an estimative of NPs production volumes, application method, and end-of-life. In addition, it also considered the mass released to the atmosphere, water, and soil.

Figure 3.1 presents the biometric parameters and chlorophyll content of soybean plants exposed to Ce NPs and $Ce(NO_3)_{3(aq)}$. The results showed that $Ce(NO_3)_{3(aq)}$ and Ce NPs in all doses (0.05 and 0.75 mg L^{-1}) did not affect soybean plant height, number of leaves, and chlorophyll content (Figure 3.1a-c). The treatments did not affect the grain yield, number of pods, average number of seeds, and average seed dry mass (Figure 3.1d) were not statistically different from the control under the Tukey test at 95 % confidence level. It is important to emphasize that the concentration of treatments was maintained in throughout the experiment.

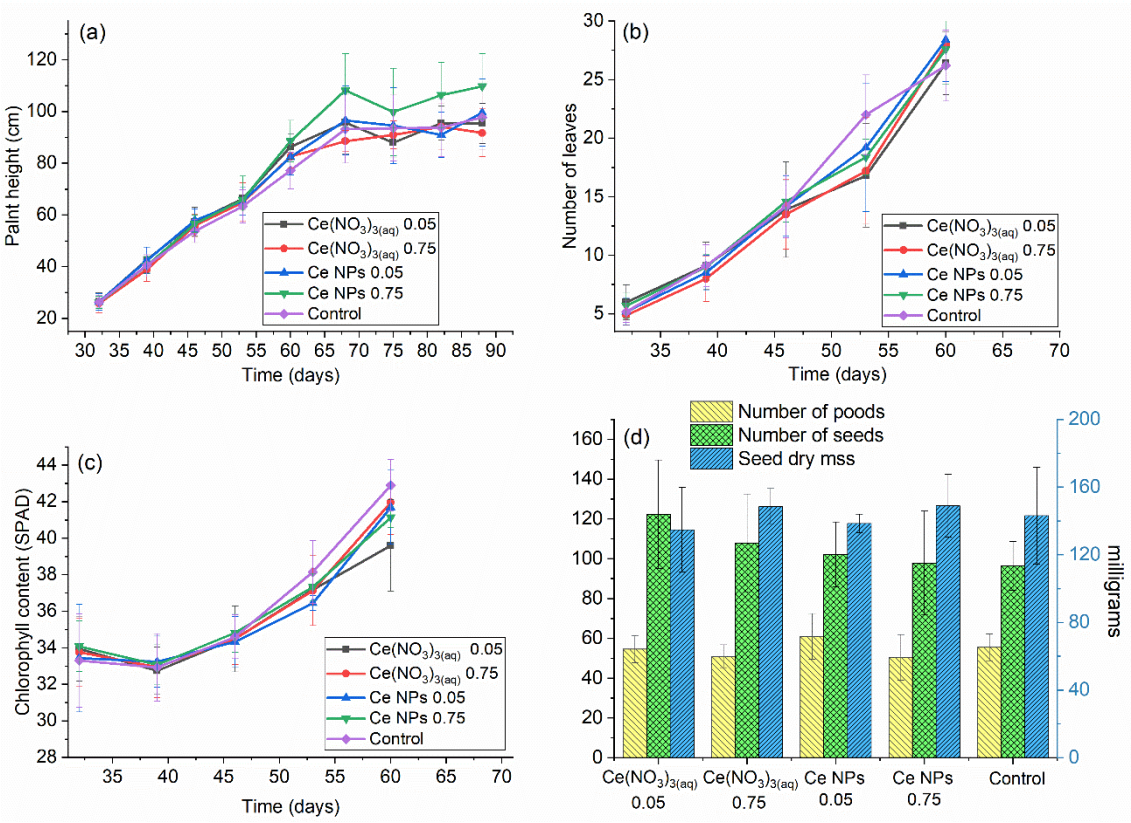

Figure 3.1. Biometric parameters and chlorophyll content of soybean (*Glycine max* L.) plants treated with 25 nm Ce NPs and $Ce(NO_3)_{3(aq)}$ at 0.05 and 0.75 mg L^{-1}; (a) plant height, (b) number of leaves, (c) chlorophyll relative content and (d) yield data (number of pods, average number of seeds and average seed dry mass for each treatment). The measurements were carried out in quintuplicate. No statistical difference was observed, for any evaluated parameter, under the Tukey test at 95% confidence level

The bibliographic survey presented in Table 3.1 shows results of several studies in which plants were exposed to Ce NPs via root system. Morphological alterations were just noticed at above *ca*. 100 mg kg^{-1}, and most of the reported effects are detrimental. This evidences the scarcity of studies involving the use of realistic concentrations of Ce NPs.

Although this experiment was conducted under hydroponic conditions, here we showed evidence that the concentration of Ce NPs estimated to 2050 (GIESE et al., 2018) in agricultural and sludge treated soils might not interfere with the soybean grain yield and morphological parameters here evaluated.

On the other hand, µ-XRF line scans in the root of treated plants (Figure 3.2) showed the presence of Ce in the inner root tissue, indicating that soybean plants can take up Ce from soluble and nanoparticle form. However, it is worth mentioning that the intensity of Ce (which is directly proportional to its concentration) was more pronounced in the root epidermis and vessel element lumen for both Ce NPs (Figure 3.2 a) and Ce $(NO_3)_3$ (Figure 3.2 b) treatments.

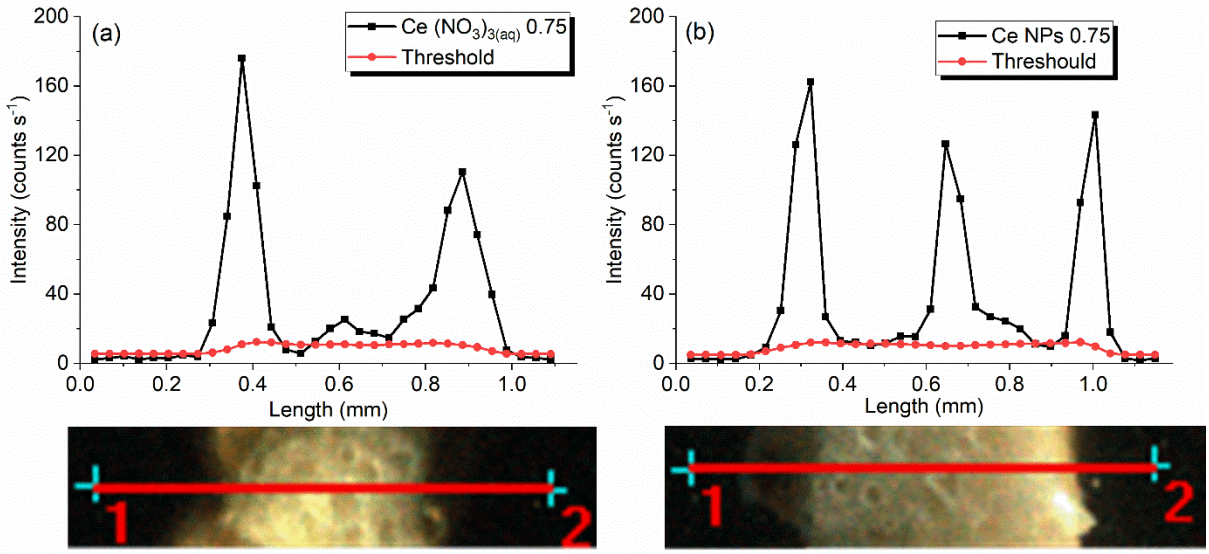

Figure 3.2. Line scan monitoring of Ce by µ-XRF in cross sectioned soybean (*Glycine max* L.) roots treated with (a) $Ce(NO_3)_{3(aq)}$ 0.75 and (b) Ce NPs 0.75, both at 0.75 mg L^{-1}, and their corresponding optical images (below). The threshold indicated the instrumental limit of detection (8.45 sigma). Cerium was found along the whole cross sections of the roots, but its intensity was more pronounced at the epidermis region for both treatments

The fact that NPs present excellent adsorption properties (CUI et al., 2018) can explain the higher intensity of Ce in the root surface. We suppose that the particles, as well was ions, are physically bound to the mucilage. Higher Ce content in the root surface was also reported in maize (*Zea mays*) (ZHAO et al., 2012) and radish (*Raphanus sativus* L) (WOJCIESZEK et al., 2019) roots exposed to CeO_2 NPs. Similar results were also reported for plants exposed to carbon nanotubes (*Oryza sativa* L. ssp.) (LIN et al., 2009), Ag NPs (*Arabidopsis thaliana*) (BAO; OH; CHEN, 2016) and some micronutrients such as Zn (*Lolium perenne*) (LIN; XING, 2008), Cu (*Triticum aestivum* L.) (DIMKPA et al., 2013) and Fe (*Hordeum vulgare* L.) (TOMBULOGLU et al., 2019) in NPs form.

Cerium presence was not only restricted to the inner root, it was also found in shoot and even grains in all Ce treatments. Figure 3.3 (a) shows that the concentration and accumulation of Ce in treated soybean shoot was depended on the applied source, but not did not vary as a

function of the concentration. The concentration and accumulation of Ce in the $Ce(NO_3)_{3(aq)}$ treatment at 0.05 mg L^{-1} was ca. 10 and 25-fold times higher, respectively, than 25 nm Ce NPs treatment at 0.75 mg L^{-1} of Ce, after 15 days of exposure.

Conversely, Figure 3.3 (b) shows that in grains, neither the source nor the concentration affected the concentration and accumulation of Ce according to the Tukey test at 95% confidence interval. Hernandez-Viezcas et al., (2013) too evidenced CeO_2 in the pod of soybean plant cultivated in soil treated with CeO_2 (8nm) at 1000 mg kg^{-1} by μ-XANES analysis (micro- X-ray absorption near-edge structure).

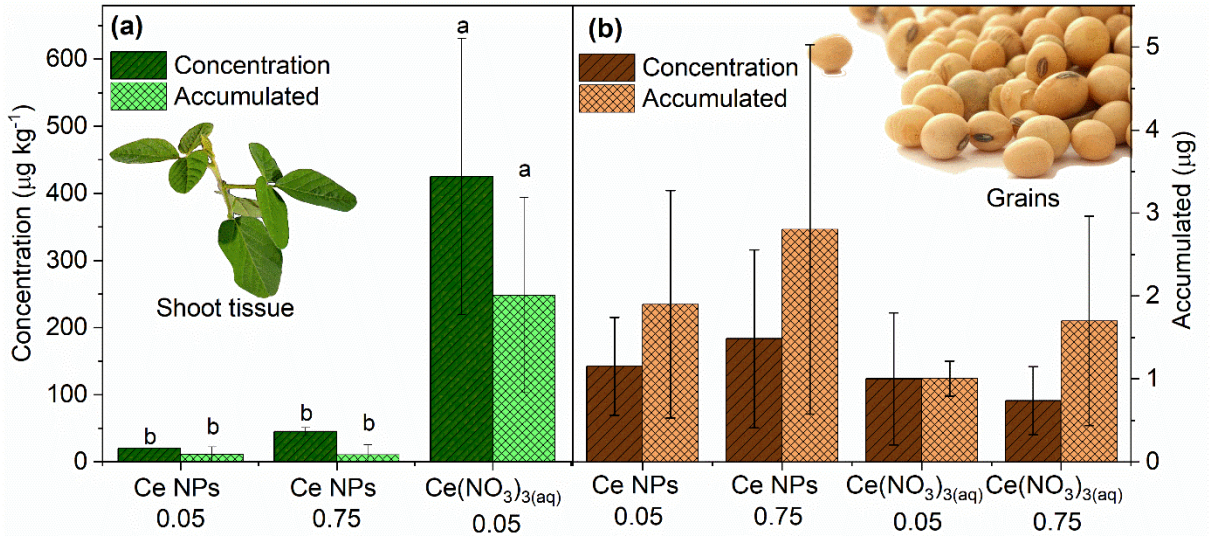

Figure 3.3. Cerium concentration and accumulation in shoot and grain of the soybeans (*Glycine max* L.) plants exposed to the 25 nm Ce NPs at 0.05 and 0.75 mg L^{-1}, and $Ce(NO_3)_{3(aq)}$ at 0.05 mg L^{-1} for 15 days. The average accumulation of Ce was estimated considering the total mass of the shoot and grain of each replicate. The absorption and translocation of Ce NPs from root to the shoot was evident, but much lower than the values for Ce soluble form (ca. 10-fold lower) (a). The data revealed that soybean plants were able to uptake Ce NPs and to translocate it from root to grains, although no statistical difference was observed under the Tukey test at 95% confidence level (b). The same lower case letters indicate no statistical difference under the Tukey test at 95% confidence level. The experiment was carried out in quintuplicate However the replicates of treatment that showed analytical signals below the average of negative control were removed from the statistical analysis. The average concentration of Ce detected in the control group was 68±23 μg kg^{-1} and 79±55 μg kg^{-1} in shoot and grain, respectively, these values were subtracted from the Ce concentration obtained for the treatments.

The trueness of analytical method was verified with spike in control sample. The recovery was between 93 to 107% of spike (Table 3.5)

Table 3.5. The analytic trueness verified by spike in control grain and leaf

Sample Id	Waited concentration (ug kg^{-1})	Concentration (ug kg^{-1})	Recuperation (%)
Spike in leaf	0.52	0.570	107.3
Spike in grain 1	0.0099	0.009	93.3
Spike in grain 2	0.050	0.049	95.1
Spike in grain 3	0.51	0.501	98.5

Since Ce was found in the grains, it is important to emphasize the lack of knowledge about the effects of Ce in human health and limits of acceptable Ce concentration in staple food. Several authors have expressed concern about this matter (MIRALLES; CHURCH; HARRIS, 2012; SCHWAB et al., 2015; TURRA, 2018; WANG et al., 2012a; ZHANG et al., 2015; ZHAO et al., 2012).

Nearly 80% of processed soybean grains are converted into soybean meal while 20 % becomes oil (BERK, 1992) This soybean meal is the major source of protein for animal feed. For pigs, the conversion ratio from feed to meet is in average 3.28 kg of feed to 1 kg of live body weight in growing or finisher phase (LOSINGER, 1998). Usually, pig feed contains *ca*. 16% of protein mostly from soybean meal (*ca*. 44% of protein) (EMBRAPA, 2003). Hence, if the grains harvested in this study were used to produced animal feed, the soybean meal would contain 137.5 µg Ce per kg of soybean meal. Supposing a scenario of biomagnification, in which all Ce present in soybean meal would be accumulated in the pig meat, and considering the conversions stated above, the pig meat could contain up to 204.4 µg Ce per kg of meat.

It is important to emphasize that we did not find any study covering health hazard assessments for human Ce oral exposition (USEPA, 2009). Gómez-Aracena et al. (2006) found correlation between Ce concentration and risk of a first acute myocardial infarction. The mean concentration founded in toenail was 186 µg kg^{-1}. This fact increases the concern about the insertion of Ce into the food chain.

Figure 3.4 shows the Ce concentration in soybean leaves that was weekly measured during 4 weeks in plants exposed to 25 nm Ce NPs and $Ce(NO_3)_{3(aq)}$ at 0.75 mg L^{-1}. The Ce concentration from soluble Ce treatment constantly increased along the four weeks, reaching a figure ca. 10-fold higher than in the first week of measurement. On the other hand, the concentration of Ce in NPs treatment did not change during the first two weeks, then decreased by half within the next two weeks. The differences between the treatments can be assigned to the distinct solubilities of the Ce sources.

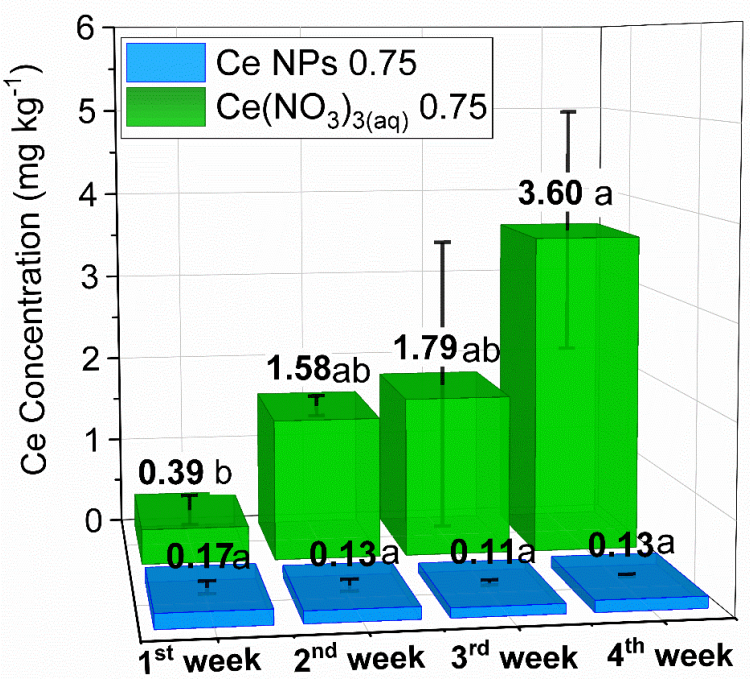

Figure 3.4. Cerium concentration in soybean (*Glycine max* L.) leaves measured along 4 weeks (once a week) of plant exposure to 25 nm Ce NPs and $Ce(NO_3)_{3(aq)}$ at 0.75 mg L^{-1}. A weekly increase of Ce was observed for the soluble Ce treatment. For 25 nm Ce NPs, Ce levels in leaves remained constant during the first two weeks, then decreased by half within the next two weeks. The same lower-case letters indicate no statistical difference under the Tukey test at 95% confidence level.

The normalized frequency shown in figures 3.5, 3.6 and 3.7 means that the size frequency was normalized by total sum of signal of each biological replicate. The frequency is defined by number of NPs of same size were measured by equipment. Therefore, the SP-ICP-MS analysis provided evidence that soybean was able to uptake Ce NPs in the nanoparticle form and translocate it from root to shoot (Figure 3.5). We found clusters with 40 and 31 nm of diameter in the first three weeks (Figure 3.5 a-c) and in the fourth week (Figure 3.5 d) of exposure, respectively. Similar average size distributions were found in the control samples spiked with Ce NPs after enzymatic digestion (right before analysis) and before the sample preparation steps (enzymatic digestion and cryogenic grinding). In these samples, Ce NPs sizes ranged between 30 - 45 nm and 35 - 45 nm, respectively (Figure 3.6 a and b). These results indicate that digestion procedure did not affect the size of NPs. In addition, negative control and soluble Ce treatment were also analyzed by SP-ICP-MS. However, the negative control (Figure 3.7) did not show a regular distribution, whereas in the soluble Ce (Figure 3.8) the size histogram did not present the same shape and average nanoparticle size of the both spiked samples (Figure 3.6 a and b).

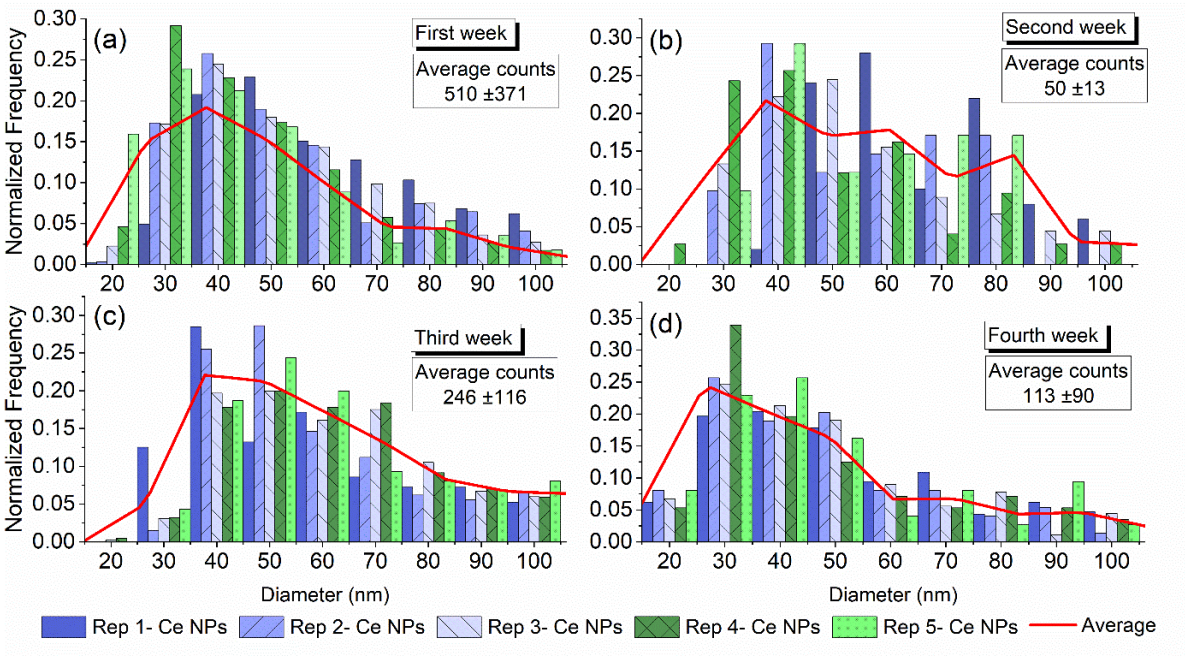

Figure 3.5. Size distribution histograms of Ce NPs in the leaves of soybean (*Glycine max*. L.) plants exposed to 25 nm Ce NPs. The measurements were carried out once a week with five biological replicates (a-d). The range of Ce NPs size varied between 25 and 55 nm. The red lines indicate five and two replicates

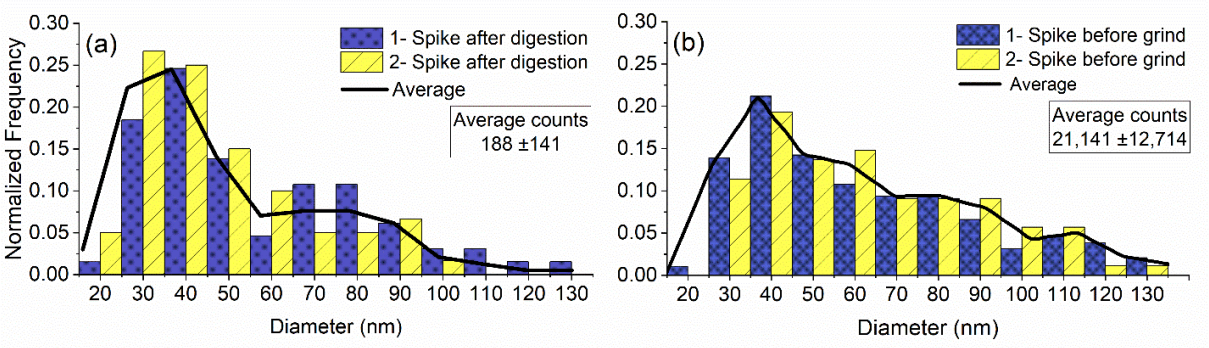

Figure 3.6. The effect of sample preparation on NPs Ce was evaluated by spiking Ce NPs in control sample before cryogenic grinding and enzymatic digestion (a-b). This latter assay was carried out in two biological duplicates. The Ce spiking histogram presented a particle size range from 25 to 55 nm. The black lines indicate five and two replicates

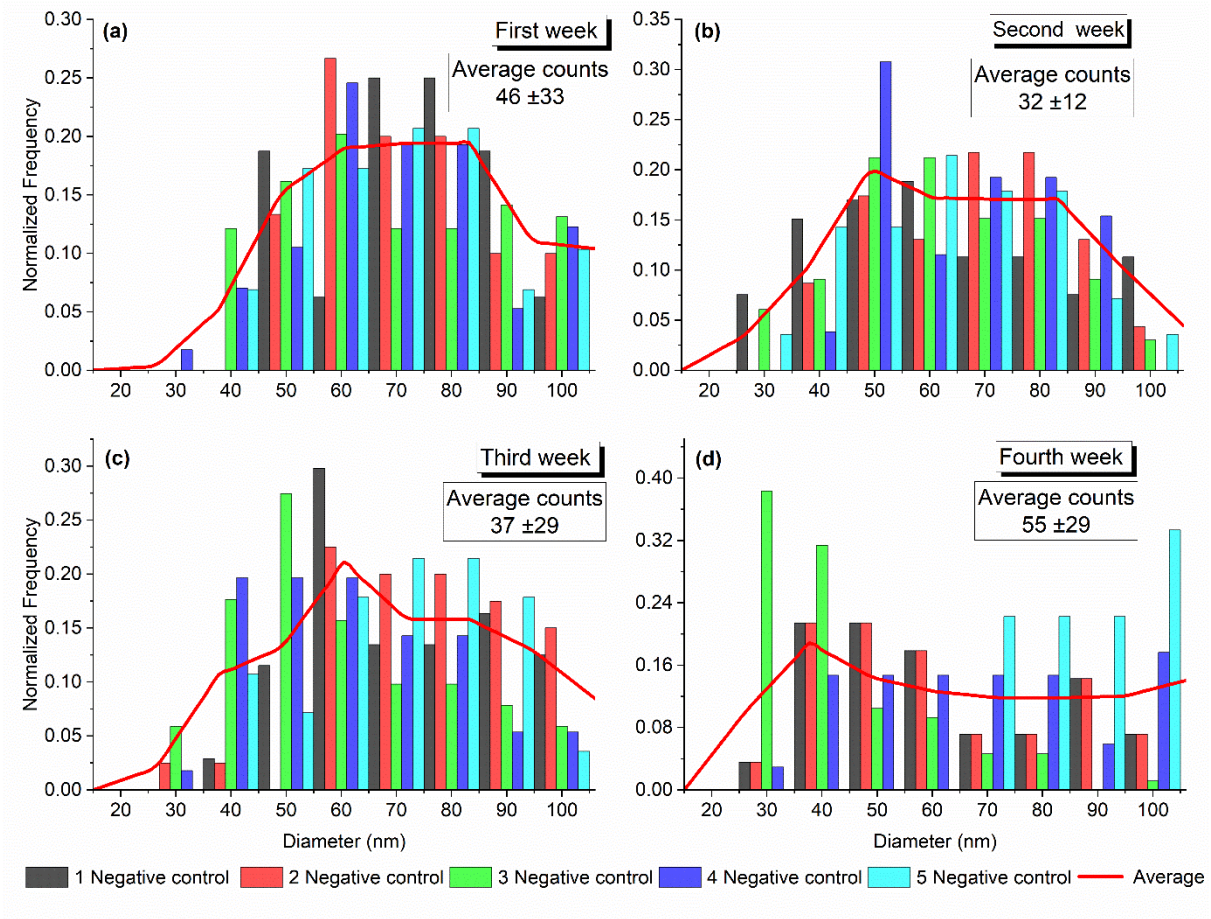

Figure 3.7. Size distribution histograms of searching for Ce NPs in the leaves of soybean (Glycine max L.) plants not exposed to nanoparticles (negative control). The measurements were carried out once a week with five biological replicates (a-d). The red lines indicate the average of the five replicates. It was not noted the normal distribution in the histogram.

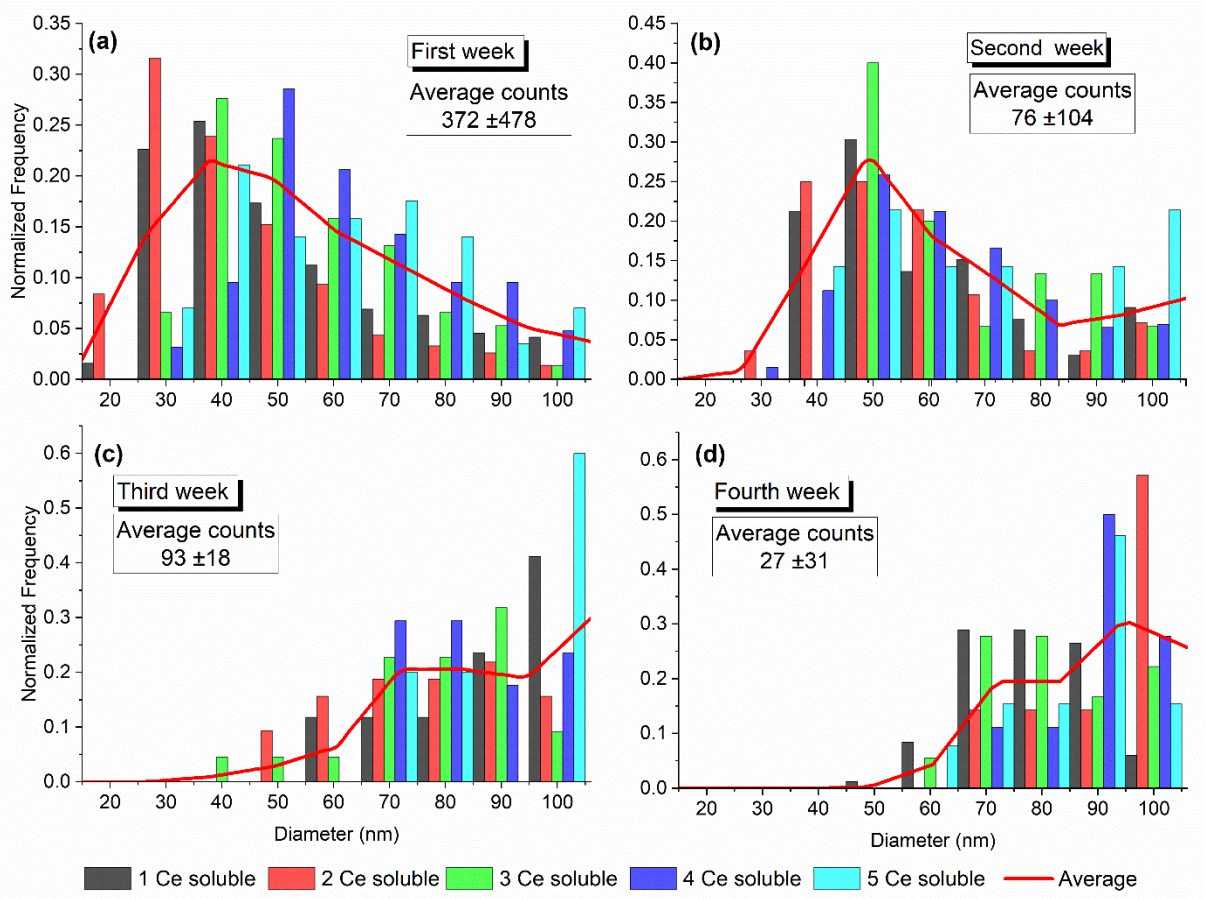

Figure 3.8. Size distribution histograms of Ce NPs in the leaves of soybean (*Glycine max* L.) plants exposed to $Ce(NO_3)_{3(aq)}$. The measurements were carried out once a week with five biological replicates (a-d). The red lines indicate the average of the five replicates. It was not noted the normal distribution in the histogram.

Although it is still not clear how plant absorb NPs by roots, several hypotheses and mechanisms have been proposed. It has been shown that nanoparticles such as ZnO are dissolved in the rhizosphere and then absorbed and transported in ionic form (DA CRUZ et al., 2017; 2019). Similarly, it has been proposed that low solubility NPs, such as CeO_2, can be partially dissolved by roots exudates such as organic acid and sugars (BAIS et al., 2006; MA et al., 2015; WANG et al., 2012b; ZHANG et al., 2012).

Also, The NPs adsorbed on the root surface might be incorporated into the cell wall and then enter the cell (KHAN et al., 2019; ZHANG et al., 2011). Endocytosis has been suggested as the process of internalization of NPs in plant cell after crossing the cell wall (SCHWAB et al., 2015). This process was observed in *Arabidopsis thaliana* exposed to CeO_2 NPs (YANG et al., 2017) and carbon nanotubes (SHEN et al., 2010), in tobacco (*Nicotiana tabacum*) exposed to Au NPs (ONELLI et al., 2008) and also in rice exposed to carbon nanotubes (SHEN et al., 2010).

There is also evidences that NPs can pass through the pores in the cell wall entirely, nonetheless, in this pathway the entrance of particles is limited by the size of the pores (*ca*.3.5–5 nm) (CARPITA et al., 1979; SCHWAB et al., 2015). Another study suggested that the uptake of NPs can occur by the root apex, more specifically in the meristematic tissue below the root cap, a region with intense cell division activity, and therefore a porous tissue (LV et al., 2015; WANG et al., 2012b). Besides that, the Casparian strips are not fully developed in this region which allows the NPs to reach the plant conductive systems easier (FELLOWS; WANG; AINSWORTH, 2003).

It is still not clear how NPs cross the Casparin strip and reach the vessel systems, nonetheless, the translocation of Ce NPs was reported to be carried out by the xylem, driven by the transpiration stream following the water flow (ZHAO et al., 2012). The capacity of plants to translocate Ce NPs from root to shoot was already demonstrated for radish (*Raphanus sativus* L.) (WOJCIESZEK et al., 2019), cucumber (*Cucumis sativus* L.) (ZHANG et al., 2012, 2011), tomato (*S. lycopersicum* L.), pumpkin (Cucurbita pepo), and soybean (*Glycine max* L.) (DAN et al., 2016), in *Arabidopsis thaliana* (YANG et al., 2017), and in lettuce (ZHANG et al., 2017).

Into the plant tissues NPs tend to form clusters, increasing their average size. Wojcieszek et al. (2019) found Ce NPs clusters with an average size of 60.3 nm into the shoot of radish (*Raphanus sativus L.*) treated with 30-50 nm Ce NPs. Similarly, the average size of Ce NPs found within roots of our soybean plants exposed to 25 nm Ce NPs was also higher than the applied size.

3.4 Conclusion

The employed cerium concentrations of at 0.05 and 0.75 mg L^{-1} (corresponding to 0.062 and 0.93 mg kg^{-1} of CeO_2, respectively) aimed at mimicking the upper threshold environmental concentration of CeO_2 nanoparticles that may exist in 2050.The present study concludes that the evaluated biometric parameters of soybean plants exposed to 25 nm CeO_2 did not present any difference from control plants. Similarly, the grain yield was not affected by the CeO_2 NPs treatments. Plants were not affected either by the $Ce(NO_3)$ employed as positive control. Thus, neither phytotoxicity by cerium ions or nano phytotoxicity was found in the present study.

We must acknowledge that soils are a much more complex environment than hydroponic solution. We believe that if CeO_2 NPs could impact the microbial community, *eg*. nitrifying bacteria and mycorrhizae, this ultimately would affect the soybean development. Thus, soil studies under realistic predicted CeO_2 NPs concentration must be carried out.

Also, we confirmed that even at low concentrations, soybean plants can take up and translocate Ce from root up to grains. This increases the concern about the insertion introduction of Ce into the food chain, whose possible consequences still needs must to be investigated.

In agreement with previous studies, we found that soybean can take up entire CeO_2 nanoparticles. However, the long-term experiment (kinetics) showed that the concentration of CeO_2 NP does not increase as function of time. This suggests that the CeO_2 is transported by mass flow whose flux increases according to the biomass production. On the other hand, the concentration of Ce from $Ce(NO_3)$ increased while the biomass production was not compromised. This indicates that ionic and nanoparticulate cerium assume different routes of assimilation in the plant.

Finally, SP-ICP-MS results revealed that the cerium found in the shoot of plants exposed to CeO_2 NPs are constituted of nanoparticles while cerium found in the shoot of plants exposed to $Ce(NO_3)_3$ present a different pattern. Hence, these results combined to evolution of cerium concentration in the shoot as function of time, suggest that CeO_2 NPs are absorbed in pristine form (entirely) as well as dissolved.

4 FINAL REMARKS AND OUTLOOK

The investigation of rare earth elements effect on the soybean plant, here presented in two different approaches (foliar and root application) allowed us to draw some conclusions. The positive effects showed in the research previously cited here were not reproduced in both experiments. Since the foliar application caused phytotoxic effects due to the high concentration of the solution. The symptoms were like some micronutrients when applied at high concentration. However, this effect did not cause alteration in the development or in the production of soybean grain. It is important to emphasize that the experiments were conducted under laboratory conditions.

The results of REE quantification in grain indicate that, both elements (lanthanum and cerium) were translocated to grain. The foliar application experiment showed that translocation of La was dose-dependent though it was not linear, which indicates that others factors might influence its translocation form leaf to grain. Conversely, the translocation of Ce from root to grain was neither dose nor compound form dependent (soluble or nanometric), since the concentration founded in grain was not statistically different between treatments (experiment developed with realistic concentration predicted to 2050).

The Ce kinetic study from root to shoot showed distinct result between soluble and nanometric form. Since, soluble form was time dependent while the concentration in shoot of plant treated with Ce NPs did not change as a function of the time. Besides that, SP-ICP-MS analysis confirmed that soybean plant is able to uptake and translocate CeO_2 NPs in pristine form.

Much attention must be paid to the introduction of REE in chain food. Differently from some well-known potentially toxic elements, such as Hg and Pb, the REE do not have a comprehensive legislation or toxicological studies stablishing acceptable levels of these element in environment, water or food. We must keep in mind that the industrial usage of REE is increasing. Further investigations are necessary since the results here presented concern only for the effect on soybean plant development and production under laboratory condition.

REFERENCES

ABREU, V. A. de. **Investigação Prospectiva na Indústria dos Terras Raras. Subsídio para políticas e gestão em minerais/materiais estratégicos**. 1991. 139 p. Dissertação (Mestrado) - Instituto de Geociencias, Universidade Estadual de Campinas, Campinas, 1991. Disponível em: <http://repositorio.unicamp.br/jspui/handle/REPOSIP/287492>.

ADAMS, C. M.; CAPORN, S. J. M.; HUTCHINSON, T. C. Crystal occurrence and wax disruption on leaf surfaces of cabbage treated with simulated acid rain. **New Phytologist**, v. 114, n. 1, p. 147–158, 1990.

ADISA, I. O. et al. Role of cerium compounds in fusarium wilt suppression and growth enhancement in tomato (*Solanum lycopersicum*). **Journal of Agricultural and Food Chemistry**, v. 66, n. 24, p. 5959–5970, 2018.

AGATHOKLEOUS, E.; KITAO, M.; CALABRESE, E. J. The rare earth element (REE) lanthanum (La) induces hormesis in plants. **Environmental Pollution**, v. 238, p. 1044–1047, 2018.

BAIS, H. P. et al. The role of root exudates in rhizosphere interactions with plants and other organisms. **Annual Review of Plant Biology**, v. 57, n. 1, p. 233–266, 2006.

BAO, D.; OH, Z. G.; CHEN, Z. Characterization of Silver Nanoparticles Internalized by Arabidopsis Plants Using Single Particle ICP-MS Analysis. **Frontiers in Plant Science**, v. 7, p. 32, 2016.

BERK, Z. **Technology of production of edible flours and protein products from soybeans.** Rome: FAO, 1992. (Agricultural Services Bulletin, 97).

BICKFORD, C. P. Ecophysiology of leaf trichomes. **Functional Plant Biology**, v. 43, n. 9, p. 807, 2016.

CAKMAK, I.; MARSCHNER, H. Increase in Membrane Permeability and Exudation in Roots of Zinc Deficient Plants. **Journal of Plant Physiology**, v. 132, n. 3, p. 356–361, 1988.

CAO, Z. et al. Physiological effects of cerium oxide nanoparticles on the photosynthesis and water use efficiency of soybean (Glycine max (L.) Merr.). **Environmental Science: Nano**, v. 4, n. 5, p. 1086–1094, 2017.

CARPITA, N. et al. Determination of the Pore Size of Cell Walls of Living Plant Cells. **Science**, v. 205, n. 4411, p. 1144–1147, 1979.

CARVALHO, F. P. Mining industry and sustainable development: time for change. **Food and Energy Security**, v. 6, n. 2, p. 61–77, maio 2017.

CUI, D. et al. Effect of cerium oxide nanoparticles on asparagus lettuce cultured in an agar medium. **Environmental Science: Nano**, v. 1, n. 5, p. 459–465, 2014.

CUI, Z. et al. Size-Dependent Thermodynamics and Kinetics of Adsorption on Nanoparticles: A Theoretical and Experimental Study. **Langmuir**, v. 34, n. 10, p. 3197–3206, 13 mar. 2018.

DA CRUZ, T. N. M. et al. Shedding light on the mechanisms of absorption and transport of ZnO nanoparticles by plants: via in vivo X-ray spectroscopy. **Environmental Science: Nano**, v. 4, n. 12, p. 2367–2376, 2017.

DA CRUZ, T. N. M. et al. A new glance on root-to-shoot in vivo zinc transport and time-dependent physiological effects of ZnSO4 and ZnO nanoparticles on plants. **Scientific Reports**, v. 9, n. 1, p. 1–12, 2019.

DAMATO, T. C. et al. The interactions between surfactants and the epicuticular wax on soybean or weed leaves: Maximal crop protection with minimal wax solubilization. **Crop Protection**, v. 91, p. 57–65, 2017.

DAMHUS, T.; HARTSHORN, R. M.; HUTTON, A. T. Nomenclature of inorganic chemistry: IUPAC recommendations 2005. **CHEMISTRY International**, 2005.

DAN, Y. et al. Characterization of gold nanoparticle uptake by tomato plants using enzymatic extraction followed by single-particle inductively coupled plasma-mass spectrometry analysis. **Environmental Science and Technology**, v. 49, n. 5, p. 3007–3014, 2015.

DAN, Y. et al. Single particle ICP-MS method development for the determination of plant uptake and accumulation of CeO2 nanoparticles. **Analytical and Bioanalytical Chemistry**, v. 408, n. 19, p. 5157–5167, 2016.

DE OLIVEIRA, C. et al. Bioaccumulation and effects of lanthanum on growth and mitotic index in soybean plants. **Ecotoxicology and Environmental Safety**, v. 122, p. 136–144, dez. 2015.

DIATLOFF, E.; ASHER, C. J.; SMITH, F. W. Foliar application of rare earth elements to maize and mungbean. **Australian Journal of Experimental Agriculture**, v. 39, n. 2, p. 189, 1999a.

DIATLOFF, E.; ASHER, C. J.; SMITH, F. W. The Effects of Rare Earth Elements on the Growth and Nutrition of Plants. **Materials Science Forum**, v. 315–317, p. 354–360, 1999b.

DIATLOFF, E.; SMITH, F. W.; ASHER, C. J. Effects of lanthanum and cerium on the growth and mineral nutrition of corn and mungbean. **Annals of Botany**, v. 101, n. 7, p. 971-982, 2008.

DIMKPA, C. O. et al. Fate of CuO and ZnO nano- and microparticles in the plant environment. **Environmental Science and Technology**, v. 47, n. 9, p. 4734–4742, 2013.

DJINGOVA, R. et al. Multielement Analytical Spectroscopy in Plant Ionomics Research. **Applied Spectroscopy Reviews**, v. 48, n. 5, p. 384–424, jul. 2013.

DU, W. et al. Physiological and biochemical changes imposed by CeO2 nanoparticles on wheat: a life cycle field study. **Environmental Science and Technology**, v. 49, n. 19, p. 11884–11893, 2015.

DUKHNYTSKYI, B. World agricultural production. **Ekonomika APK**, n. 7, p. 59–65, 2019.

EMBRAPA. **Produção de suínos**. Concórdia: Embrapa Suínos e Aves, 2003. Disponível em: <http://www.cnpsa.embrapa.br/SP/suinos/nutricao.html>. Acesso em: 23 out. 2019.

EMBRAPA. **Soja em números**. Londrina: Embrapa Soja, 2019. Disponível em: <https://www.embrapa.br/web/portal/soja/cultivos/soja1/dados-economicos>.

ESPINDOLA, M. C. G.; DE MENEZES, N. L.; BARBIERI, A. P. P. Efeito do cério na qualidade fisiológica de sementes de milho e no desempenho agronômico das plantas. **Bioscience Journal**, v. 29, n. 5, p. 1501–1507, 2013.

EUROPEAN AGENCY FOR SAFETY AND HEALTH AT WORK. **Foresight of new and emerging risks to occupational safety and health associated with new technologies in green jobs by 2020** - Phase II – Key Technologies. Bilbao, 2011. 50 p.

EUROPEAN AGENCY FOR SAFETY AND HEALTH AT WORK. **Priorities for occupational safety and health research in Europe**: 2013-2020. Luxembourg: Publications Office of the European Union, 2013. doi: 10.2802/25457.

FAGERIA, N. K. et al. Foliar fertilization of crop plants. **Journal of Plant Nutrition**, v. 32, n. 6, p. 1044–1064, 2009.

FASHUI, H. et al. The effect of cerium (III) on the chlorophyll formation in spinach. **Biological Trace Element Research**, v. 89, n. 3, p. 263–276, 2002.

FELLOWS, R. J.; WANG, Z.; AINSWORTH, C. C. Europium uptake and partitioning in oat (Avena sativa) Roots as studied by laser-induced fluorescence spectroscopy and confocal microscopy profiling technique. **Environmental Science & Technology**, v. 37, n. 22, p. 5247–5253, 2003.

FERNÁNDEZ, V.; EBERT, G. Foliar Iron Fertilization: A Critical Review. **Journal of Plant Nutrition**, v. 28, n. 12, p. 2113–2124, 2005.

FERNÁNDEZ, V.; SOTIROPOULOS, T.; BROWN, P. **Adubação foliar**: fundamentos científicos e técnicas de campo. São Paulo: Abisolo, 2015. 152 p.

FINK, G. Encyclopedia of the Elements. Technical Data, History, Processing, Applications. Von Per Enghag. **Angewandte Chemie**, v. 117, n. 21, p. 3236–3237, 2005.

GANGULI, R.; COOK, D. R. Rare earths: A review of the landscape. **MRS Energy & Sustainability**, v. 5, E9, 2018. Disponível em: https://www.cambridge.org/core/product/identifier/S2329222918000077/type/journal_article.

GAO, Y. et al. Effects of LaCl3 on the growth and photosynthetic characteristics of Fny-infected tobacco seedlings. **Journal of Rare Earths**, v. 30, n. 7, p. 725–730, 2012.

GIESE, B. et al. Risks, release and concentrations of engineered nanomaterial in the environment. **Scientific Reports**, v. 8, n. 1, p. 1565, 2018.

GÓMEZ-ARACENA, J. et al. Toenail cerium levels and risk of a first acute myocardial infarction: The EURAMIC and heavy metals study. **Chemosphere**, v. 64, n. 1, p. 112–120, 2006.

GUI, X. et al. Fate and phytotoxicity of CeO2 nanoparticles on lettuce cultured in the potting soil environment. **PLoS ONE**, v. 10, n. 8, p. 1–10, 2015.

GUI, X. et al. Phytotoxicity of CeO2 nanoparticles on radish plant (Raphanus sativus). **Environmental Science and Pollution Research**, v. 24, n. 15, p. 13775–13781, 2017.

HAGEDORN, O. et al. Surfactant-induced enhancement of droplet adhesion in superhydrophobic soybean (Glycine max L.) leaves. **Beilstein Journal of Nanotechnology**, v. 8, n. 1, p. 2345–2356, 8 nov. 2017.

HAMIDREZA, S.; XIAOXUAN, W.; XINGMAO, M. Impact of nanoparticle surface charge and phosphate on the uptake of coexisting cerium oxide nanoparticles and cadmium by soybean (Glycine max (L.) Merr.). **International Journal of Phytoremediation**, 2019. Disponível em: <https://doi.org/10.1080/15226514.2019.1658713>.

HAYNES, W. M. **CRC handbook of chemistry and physics**. Boca Raton: CRC Press, 2014.

HAZEN, J. L. **Adjuvants**: terminology, classification, and chemistry. **Weed Technology**, v. 14, n. 4, p. 773–784, 2000. Disponível em: http://www.jstor.org/stable/3988668.

HERNANDEZ-VIEZCAS, J. A. et al. In situ synchrotron X-ray fluorescence mapping and speciation of CeO 2 and ZnO nanoparticles in soil cultivated soybean (Glycine max). **ACS Nano**, v. 7, n. 2, p. 1415–1423, 2013.

HOAGLAND, D. R.; ARNON, D. I. **The water-culture method for growing plants without soil**. 2. ed. Berkeley, CA: California Agricultural Experiment Station, 1950. (Circular, 347).

HONG, F. Mechanism of lanthanum effect on chlorophyll of spinach. **Science in China Series C**, v. 45, n. 2, p. 166, 2002.

HONG, F.; QU, C.; WANG, L. Cerium improves growth of maize seedlings via alleviating morphological structure and oxidative damages of leaf under different stresses. **Journal of Agricultural and Food Chemistry**, v. 65, n. 41, p. 9022–9030, 2017.

HU, X.; WANG, X.-R.; WANG, C. Bioaccumulation of Lanthanum and Its Effect on Growth of Maize Seedlings in a Red Loamy Soil. **Pedosphere**, v. 16, n. 6, p. 799–805, 2006.

HUANG, G.; WANG, L.; ZHOU, Q. Lanthanum (III) Regulates the Nitrogen Assimilation in Soybean Seedlings under Ultraviolet-B Radiation. **Biological Trace Element Research**, v. 151, n. 1, p. 105–112, 2013.

IPPOLITO, M. P. et al. Responses of antioxidant systems to lanthanum nitrate treatments in tomato plants during drought stress. **Plant Biosystems - An International Journal Dealing with all Aspects of Plant Biology**, v. 145, n. 1, p. 248–252, 2011.

KARNOVSKY, M. J. A formaldehyde glutaraldehyde fixative of high osmolality for use in electron microscopy. **Journal of Cell Biology**, v. 27, p. 1A-149A, 1965.

KHAN, M. R. et al. Nanoparticle–Plant Interactions: Two-Way Traffic. **Small**, v. 1901794, 2019. Disponível em: <https://onlinelibrary.wiley.com/doi/abs/10.1002/smll.201901794>.

LACERDA, J. J. de J. et al. Soybean yield responses to micronutrient fertilizers. In: KASAI, M. (Ed.). **Soybean -** The basis of yield, biomass and productivity. Rijeka: InTech, 2017.

LI, X. et al. Bt-transgenic cotton is more sensitive to CeO2 nanoparticles than its parental non-transgenic cotton. **Journal of Hazardous Materials**, v. 274, p. 173–180, 2014.

LIANG, C.; HUANG, X.; ZHOU, Q. Effect of cerium on photosynthetic characteristics of soybean seedling exposed to supplementary ultraviolet-B radiation. **Journal of Environmental Sciences**, v. 18, n. 6, p. 1147–1151, 2006.

LIN, D.; XING, B. Root uptake and phytotoxicity of ZnO nanoparticles. **Environmental Science and Technology**, v. 42, n. 15, p. 5580–5585, 2008.

LIN, S. et al. Uptake, translocation, and transmission of carbon nanomaterials in rice plants. **Small**, v. 5, n. 10, p. 1128–1132, 2009.

LIU, D. et al. The effects of cerium on the growth and some antioxidant metabolisms in rice seedlings. **Environmental Science and Pollution Research**, v. 19, n. 8, p. 3282–3291, 2012.

LIU, D.; LIN, Y.; WANG, X. Effects of lanthanum on growth, element uptake, and oxidative stress in rice seedlings. **Journal of Plant Nutrition and Soil Science**, v. 175, n. 6, p. 907–911, 2012.

LIU, X. et al. Effect of 4f Electron Characteristics and Alternation Valence of Rare Earths on Photosynthesis: Regulating Distribution of Energy and Activities of Spinach Chloroplast. **Journal of Rare Earths**, v. 25, n. 4, p. 495–501, 2007.

LÓPEZ-MORENO, M. L. et al. X-ray absorption spectroscopy (XAS) corroboration of the uptake and storage of ceo2 nanoparticles and assessment of their differential toxicity in four edible plant species. **Journal of Agricultural and Food Chemistry**, v. 58, n. 6, p. 3689–3693, 2010.

LÓPEZ-MORENO, M. L. et al. Evidence of the differential biotransformation and genotoxicity of ZnO and CeO2 nanoparticles on soybean (Glycine max) plants. **Environmental Science & Technology**, v. 44, n. 19, p. 7315–7320, 2010.

LOSINGER, W. C. Feed-conversion ratio of finisher pigs in the USA. **Preventive Veterinary Medicine**, v. 36, n. 4, p. 287–305, 1998.

LV, J. et al. Accumulation, speciation and uptake pathway of ZnO nanoparticles in maize. **Environmental Science: Nano**, v. 2, n. 1, p. 68–77, 2015.

MA, J. J.; REN, Y. J.; YAN, L. Y. Effects of Spray Application of Lanthanum and Cerium on Yield and Quality of Chinese Cabbage (Brassica chinensis L) Based on Different Seasons. **Biological Trace Element Research**, v. 160, n. 3, p. 427–432, 15 set. 2014.

MA, C. et al. Physiological and molecular response of arabidopsis thaliana (L.) to nanoparticle cerium and indium oxide exposure. **ACS Sustainable Chemistry and Engineering**, v. 1, n. 7, p. 768–778, 2013.

MA, Y. et al. Origin of the different phytotoxicity and biotransformation of cerium and lanthanum oxide nanoparticles in cucumber. **Nanotoxicology**, v. 9, n. 2, p. 262–270, 17 fev. 2015.

MAJUMDAR, S. et al. Exposure of cerium oxide nanoparticles to kidney bean shows disturbance in the plant defense mechanisms. **Journal of Hazardous Materials**, v. 278, p. 279–287, 2014.

MAJUMDAR, S. et al. Soil organic matter influences cerium translocation and physiological processes in kidney bean plants exposed to cerium oxide nanoparticles. **Science of the Total Environment**, v. 569–570, p. 201–211, 2016.

MAO, C. X. et al. Protective Effect of Cerium Ion Against Ultraviolet B Radiation-Induced Water Stress in Soybean Seedlings. **Biological Trace Element Research**, v. 146, n. 3, p. 381–387, 2012.

MARSCHNER, P. **Marschner's mineral nutrition of higher plants**. 3.ed. New York: Academic Press, 2011.

MIRALLES, P.; CHURCH, T. L.; HARRIS, A. T. Toxicity, Uptake, and Translocation of Engineered Nanomaterials in Vascular plants. **Environmental Science & Technology**, v. 46, n. 17, p. 9224–9239, 2012.

MORALES, M. I. et al. Toxicity assessment of cerium oxide nanoparticles in cilantro (Coriandrum sativum L.) plants grown in organic soil. **Journal of Agricultural and Food Chemistry**, v. 61, n. 26, p. 6224–6230, 2013.

NHAN, L. VAN et al. Phytotoxic mechanism of nanoparticles: Destruction of chloroplasts and vascular bundles and alteration of nutrient absorption. **Scientific Reports**, v. 5, n. 1, p. 1–13, 2015.

ONELLI, E. et al. Clathrin-dependent and independent endocytic pathways in tobacco protoplasts revealed by labelling with charged nanogold. **Journal of Experimental Botany**, v. 59, n. 11, p. 3051–3068, 2008.

PANG, X.; LI, D.; PENG, A. Application of rare-earth elements in the agriculture of china and its environmental behavior in soil. **Journal of Soils and Sediments**, v. 1, n. 2, p. 124–129, 2001.

PENG, Q.; ZHOU, Q. Antioxidant Capacity of Flavonoid in Soybean Seedlings under the Joint Actions of Rare Earth Element La(III) and Ultraviolet-B Stress. **Biological Trace Element Research**, v. 127, n. 1, p. 69–80, 2009a.

PENG, Q.; ZHOU, Q. Influence of lanthanum on chloroplast ultrastructure of soybean leaves under ultraviolet-B stress. **Journal of Rare Earths**, v. 27, n. 2, p. 304–307, abr. 2009b.

PENG, Q.; ZHOU, Q. The Endogenous Hormones in Soybean Seedlings Under the Joint Actions of Rare Earth Element La(III) and Ultraviolet-B Stress. **Biological Trace Element Research**, v. 132, n. 1–3, p. 270–277, 22 dez. 2009c.

RAI, P. K. et al. Nanoparticle-plant interaction: Implications in energy, environment, and agriculture. **Environment International**, v. 119, p. 1–19, 2018.

RAMOS, S. J. et al. Rare earth elements in raw materials and products of the phosphate fertilizer industry in South America : Content , signature , and crystalline phases. v. 168, p. 177–186, 2016.

RAVEL, B.; NEWVILLE, M. ATHENA , ARTEMIS , HEPHAESTUS : data analysis for X-ray absorption spectroscopy using IFEFFIT. **Journal of Synchrotron Radiation**, v. 12, n. 4, p. 537–541, 2005.

RAVEN, P.; EVERT, R. F.; EICHHORN, S. E. **Biologia vegetal**. 7. ed. Rio de Janeiro: Guanabara Koogan, 2014.

REN, Y. et al. Effects of mixed rare earth fertilizer on yield and nutrient quality of leafy vegetables during different seasons. **Journal of Rare Earths**, v. 34, n. 6, p. 638–643,. 2016.

RICO, C. M. et al. Effect of cerium oxide nanoparticles on the quality of rice (Oryza sativa L.) grains. **Journal of Agricultural and Food Chemistry**, v. 61, n. 47, p. 11278–11285, 2013.

RICO, C. M. et al. Cerium oxide nanoparticles impact yield and modify nutritional parameters in wheat (triticum aestivum L.). **Journal of Agricultural and Food Chemistry**, v. 62, n. 40, p. 9669–9675, 2014.

RICO, C. M.; PERALTA-VIDEA, J. R.; GARDEA-TORRESDEYA, J. L. Differential effects of cerium oxide nanoparticles on rice, wheat, and barley roots: A Fourier Transform Infrared (FT-IR) microspectroscopy study. **Applied Spectroscopy**, v. 69, n. 2, p. 287–295, 2015.

RODRIGUES, E. S. et al. Laboratory microprobe X-ray fluorescence in plant science: Emerging applications and case studies. **Frontiers in Plant Science**, v. 871, 2018. doi: 10.3389/fpls.2018.01588.

SALEHI, H. et al. Morphological, proteomic and metabolomic insight into the effect of cerium dioxide nanoparticles to Phaseolus vulgaris L. under soil or foliar application. **Science of The Total Environment**, v. 616–617, p. 1540–1551, 2018.

SANTOS, E. F. et al. Physiological highlights of manganese toxicity symptoms in soybean plants: Mn toxicity responses. **Plant Physiology and Biochemistry**, v. 113, p. 6–19, 2017.

SCHWAB, F. et al. Barriers, pathways and processes for uptake, translocation and accumulation of nanomaterials in plants – Critical review. **Nanotoxicology**, v. 10, n. 3, p. 1-22, 2015.

SCHWABE, F. et al. Influence of two types of organic matter on interaction of CeO2 nanoparticles with plants in hydroponic culture. **Chemosphere**, v. 91, n. 4, p. 512–520, 2013.

SERVIN, A. D. et al. Exposure of agricultural crops to nanoparticle CeO2 in biochar-amended soil. **Plant Physiology and Biochemistry**, v. 110, p. 147–157, 2017.

SHEN, C.-X. et al. Induction of programmed cell death in Arabidopsis and rice by single-wall carbon nanotubes. **American Journal of Botany**, v. 97, n. 10, p. 1602–1609, 2010.

SHEPHERD, T.; WYNNE GRIFFITHS, D. The effects of stress on plant cuticular waxes. **New Phytologist**, v. 171, n. 3, p. 469–499, 2006.

SHYAM, R.; AERY, N. Effect of cerium on growth, dry matter production, biochemical constituents and enzymatic activities of cowpea plants [Vigna unguiculata (L.) Walp.]. **Journal of Soil Science and Plant Nutrition**, v. 12, n. 1, p. 1–14, 2012.

SUN, Z. et al. Effects and mechanisms of the combined pollution of lanthanum and acid rain on the root phenotype of soybean seedlings. **Chemosphere**, v. 93, n. 2, p. 344–352, 2013.

TEIXEIRA, I. R. et al. Manganese and zinc leaf application on common bean grown on a "Cerrado" soil. **Scientia Agricola**, v. 61, n. 1, p. 77–81, 2004.

TOMBULOGLU, H. et al. Uptake and translocation of magnetite (Fe3O4) nanoparticles and its impact on photosynthetic genes in barley (Hordeum vulgare L.). **Chemosphere**, v. 226, p. 110–122, 2019.

TUORINIEMI, J.; CORNELIS, G.; HASSELLÖV, M. Improving the accuracy of single particle ICPMS for measurement of size distributions and number concentrations of nanoparticles by determining analyte partitioning during nebulisation. **Journal of Analytical Atomic Spectrometry**, v. 29, n. 4, p. 743–752, 2014.

TURRA, C. Sustainability of rare earth elements chain: from production to food – a review. **International Journal of Environmental Health Research**, v. 28, n. 1, p. 23–42, 2018.

TYLER, G. Rare earth elements in soil and plant systems - A review. **Plant and Soil**, v. 267, n. 1, p. 191–206, 2004.

U.S. EPA. **Toxicological review of cerium oxide and cerium compounds**. In support of summary information on the Integrated Risk Information System (IRIS). Washington, DC, 2009. (EPA/635/R-08/002F).

U.S. GEOLOGICAL SURVEY. **Mineral commodity summaries 2013**. Washington, DC, 2013. 198 p.

U.S. GEOLOGICAL SURVEY. **Mineral commodity summaries 2019**. Washington, DC, 2019. 200p. doi: 10.3133/70202434.

VANCE, M. E. et al. Nanotechnology in the real world: Redeveloping the nanomaterial consumer products inventory. **Beilstein Journal of Nanotechnology**, v. 6, n. 1, p. 1769–1780, 2015.

WANG, Q. et al. The impact of cerium oxide nanoparticles on tomato (Solanum lycopersicum L.) and its implications for food safety. **Metallomics**, v. 4, n. 10, p. 1105–1112, 2012a.

WANG, Z. et al. Xylem- and phloem-based transport of CuO nanoparticles in maize (Zea mays L.). **Environmental Science and Technology**, v. 46, n. 8, p. 4434–4441, 2012b.

WEALTH DAILY. **Special Report: Rare Earth Elements in 2016**. Disponível em: <https://www.wealthdaily.com/report/rare-earth-elements-in-2016/1712>.

WILL, S. et al. Absorption and mobility of foliar-applied boron in soybean as affected by plant boron status and application as a polyol complex. **Plant and Soil**, v. 344, n. 1–2, p. 283–293, 2011.

WOJCIESZEK, J. et al. Uptake, translocation, size characterization and localization of cerium oxide nanoparticles in radish (Raphanus sativus L.). **Science of the Total Environment**, v. 683, p. 284–292, 2019.

XIAOQING, L. et al. Effects of CeCl3 on Energy Transfer and Oxygen Evolution in Spinach Photosystem II. **Journal of Rare Earths**, v. 25, n. 5, p. 624–630, 2007.

XIE, Y. et al. Effects of cerium nitrate on the growth and physiological characteristics in Cyclocarya paliurus seedlings. **Journal of Rare Earths**, v. 33, n. 8, p. 898–904, 2015.

YANG, Q. et al. Effect of lanthanum(III) on the production of ethylene and reactive oxygen species in soybean seedlings exposed to the enhanced ultraviolet-B radiation. **Ecotoxicology and Environmental Safety**, v. 104, n. 1, p. 152–159, 2014.

YANG, X. et al. Particle-specific toxicity and bioavailability of cerium oxide (CeO2) nanoparticles to Arabidopsis thaliana. **Journal of Hazardous Materials**, v. 322, p. 292–300, 2017.

YIN, S. et al. Cerium relieves the inhibition of nitrogen metabolism of spinach caused by magnesium deficiency. **Biological Trace Element Research**, v. 132, n. 1–3, p. 247–258, 2009.

ZENG, F. L. et al. Effect of lanthanum on ion absorption in cucumber seedling leaves. **Biological Trace Element Research**, v. 78, n. 1, p. 265, 2000.

ZHANG, P. et al. Biotransformation of Ceria Nanoparticles in Cucumber Plants. **ACS Nano**, v. 6, n. 11, p. 9943–9950, 2012.

ZHANG, P. et al. Phytotoxicity, uptake and transformation of nano-CeO2 in sand cultured romaine lettuce. **Environmental Pollution**, v. 220, p. 1400–1408, 2017.

ZHANG, W. et al. Uptake and accumulation of bulk and nanosized cerium oxide particles and ionic cerium by radish (Raphanus sativus L.). **Journal of Agricultural and Food Chemistry**, v. 63, n. 2, p. 382–390, 2015.

ZHANG, Z. et al. Uptake and distribution of ceria nanoparticles in cucumber plants. **Metallomics**, v. 3, n. 8, p. 816–822, 2011.

ZHAO, L. et al. Effect of surface coating and organic matter on the uptake of CeO2 NPs by corn plants grown in soil: Insight into the uptake mechanism. **Journal of Hazardous Materials**, v. 225–226, p. 131–138, 2012.

ZHU, L. et al. Effects of lanthanum on the growth and essential oil components of lavender under osmotic stress. **Journal of Rare Earths**, v. 36, n. 8, p. 891–897, 2018.

ZHUANG, M. et al. Health risk assessment of rare earth elements in cereals from mining area in Shandong, China. **Scientific Reports**, v. 7, n. 1, 2017. Disponível em: <http://www.nature.com/articles/s41598-017-10256-7>.

Foliar application of rare earth elements on soybean (Glycine max (L)): Effects on biometrics and characterization of phytotoxicity

Author:
Eduardo S. Rodrigues,Gabriel S. Montanha,João P.R. Marques,Eduardo de Almeida,Lauren N.M. Yabuki,Amauri A. Menegário,Hudson W. Pereira de Carvalho

Publication: Journal of Rare Earths

Publisher: Elsevier

Date: Available online 17 September 2019